REPUBLIQUE ALGERIENNE DEMOCRATIQUE ET POPULAIRE

MINISTERE DE L'ENSEIGNEMENT SUPERIEUR ET DE LA RECHERCHE SCIENTIFIQUE

ECOLE NORMALE SUPERIEURE DE LAGHOUAT

DEPARTEMENT : PHYSIQUE

MEMOIRE DE MAGISTER

En vue de l'obtention du diplôme de Magister en Physique

Option : Interaction champ-matière

THEME DU PROJET :

Application of machine learning methods for analyzing nondestructive testing data

Présenté par :

Mlle. Barrarat Fatima

Dirigé par :

Dr. Helifa Bachir
Dr. Rayane Karim

DEVANT LES MEMBRES DU JURY

Mr. LEFKAIER Iben Khaldoun	Professeur	Université de Laghouat	Président
Mr. BENTRIA Bachir	Professeur	Université de Laghouat	Examinateur
Mr. LAGRAA Nasreddine	Professeur	Université de Laghouat	Examinateur
Mr. HELIFA Bachir	MCA	Université de Laghouat	Directeur
Mr. RAYANE Karim	MCB	Université de Laghouat	Co-Directeur

ANNÉE UNIVERSITAIRE : 2016-2017

Acknowledgment

I want to express my appreciation and deep gratitude to Mr. Yousfi Mohamed, Professor at the University of Laghouat and the former director of the Higher Normal School of Laghouat having opened this magisterial session. Thank you, Mr YOUSFI

The work presented in this brief was carried out in the Materials Physics Laboratories (MPL), University of Laghouat.

First of all, I would like to especially thank Mr. **Iben Khaldoun Lefkaier**, Professor at the Laghouat University, Director of the MPL laboratory and responsible of our magister formation: Field-Matter Interaction at the Higher Normal School of Laghouat for the confidence he makes it welcoming me as a magister student in the MPL laboratory, and for his valuable helpers.

I would like to express my sincere thanks and my deep gratitude to the director of this brief, Mr. **Bachir Helifa**, lecturer "A" at the University of Laghouat, for his confidence, generosity, and patience, that helped me to overcome the most delicate moments of this brief. Big thanks for Mr. **Helifa**.

I want to express my appreciation and deep gratitude to the co-director of the brief, Mr. **Karim Rayane** Lecturer "B" at the University of Laghouat for providing useful suggestions throughout this work and for his advice. It is here the expression of my deep gratitude and high esteem.

I would like to thank again Mr. **Iben Khaldoun Lefkaier**, Professor at the University of Laghouat, and Director of the Materials Physics Laboratory, for honoring me to chair the jury of this brief.

I express my sincere and deep gratitude to Mr. **Bachir Bentria**, Professor at the University of Laghouat, who has done me the honor of accepting to review and evaluate this work.

I want to express my sincere gratitude to Mr. **Nasreddine Lgraa**, a lecturer at the University of Laghouat, for honoring me to accept to review and evaluate this work.

I would like to thank Mr. **Mohamed Naidjat**, a lecturer at the Higher Normal School of Laghouat, for his valuable assistance, which they have been able to bring to me for the accomplishment of this work.

I express my sincere gratitude to Mr. **Mohamed Naili**, a technician in the Electronics department laboratories at the University of Laghouat for his help.

My thanks also go to all members of the MPL laboratory. and all the staff of the graduation post of the Higher Normal School of Laghouat and specifically **Mr. Belakhdar Abdelkader**.

I address my thanks especially to my **dear parents**, who has always believed in me and gave me help and comfort, my brothers and my sisters to express my deep gratitude for their support.

Finally, I would like to thank everyone who participated in one way or another to the realization of this work.

Table of contents

General Introduction i

CHAPTER I: THE NON DESTRUCTIVE TESTING BY EDDY CURRENTS

I.1 Introduction 1
I.2 Non destructive testing methods 1
I.2.1 The various defects detected in NDT 1
I.2.1.1 The surface defects 2
I.2.1.2 The internal defects 2
I.3 Non destructive testing by eddy current 2
I.3.1 Eddy currents generation 2
I.3.2 Advantages and limits of eddy currents testing 3
a. Advantages 3
b.Limits 3
I.4 Different inductive Sensors 4
I.4.1 Dual-function sensor 4
I.4.2 Separate function sensor 4
I.5 Operating mode 4
I.5.1 Absolute mode 4
I.5.2 Differential mode 5
I.6 Excitation mode in non destructive eddy current control 5
I.6.1 Mono-frequency excitation 5
I.6.2 Multi-frequency excitation 5
I.6.3 Pulse excitation 6
I.7 Eddy currents penetration depth 6
I.8 Normalized impedance 7
I.9 Problematic of a NDT-EC system 8
I.9.1 Direct problem 9
I.9.2 Inverse problem 9
I.10 Modeling of the electromagnetic problem 9

I.10.1 Maxwell's equations 10
I.10.2 Continuity and boundary conditions 11
a. Continuity conditions 11
b. Boundary conditions 11
I.11 Formulation of the magnetodynamic problem 12
I.11.1 General formulation in potentials $(\vec{A}, V)$ 12
I.11.2 Numerical methods of discretization 13
I.11.2.1 Finite difference method (FDM) 14
I.11.2.2 Finite element method (FEM) 14
I.11.2.3 Boundary integral method (BIM) 14
I.11.2.4 Finite volume method (FVM) 15
I.11.3 Calculation of the impedance variation 15
I.11.4 Representation of eddy current signals 16
I.12 Conclusion 16

CHAPTER II: EXPERIMENTATION: TEST BENCH

II.1 Introduction 17
II.2 Impedance Diagram 17
II.3 Sensor impedance measuring equipment 18
II.3.1 Lock-in amplifier HF2LI working principle 20
II.3.2 Sensor Impedance Measurement 21
II.4 Materials to be inspected 22
II.4.1 Calibration parts qualities 22
II.4.2 Electrical discharge machining 23
II.4.2.1 EDM principle 23
II.4.2.2 Opportunities and benefits 24
II.4.3 Stallions 24
II.4.4 Sensor position relative to the sample 25
II.5 Measurement steps 26
II.5.1 Excitation 26

II.5.2 Modulation and filtering 26
II.5.3 Demodulation and visualization of the signal 26

CHAPTER III: MACHINE LEARNING APPROACHES

III.1 Introduction 27
III.2 Artificial neural networks 27
III.2.1 Formal Neuron 27
III.2.2 Transfer functions 28
a. Binary threshold function 28
b. Ramp function with saturation 28
c. Sigmoid function 28
III.2.3 Network architecture 29
III.2.3.1 Feedforward neural networks 29
a. Monolayer network 29
b. Limitation of monolayer networks 30
c. Multilayer network 30
III.2.4 Neural networks models 30
III.2.4.1 The perceptron model 30
III.2.4.2 The multilayer perceptron (MLP) 31
III.2.5 Learning neural networks 32
III.2.5.1 Supervised Learning 32
III.2.5.2 Unsupervised Learning 32
III.2.6 Learning by back-propagation algorithm 33
III.2.7 Learning Speed of neural networks 34
III.2.8 Neural network advantages and disadvantages 34
a. Advantages 34
b. Disadvantages 34
III.3 Deep learning method 35
III.3.1 Deep networks training 35
III.3.1.1 Deep network pretraining 36

III.3.1.2 Autoencoder 36
III.3.1.2.1 Autoencoder training 37
III.4 Hybrid learning method 38
III.4.1 Neuro-fuzzy networks 38
III.4.2 Fuzzy Systems 38
III.4.3 Fuzzy logic theory 39
III.4.3.1 Membership function 39
III.4.3.1.1 The membership function types 39
III.4.3.2 Fuzzy operators 41
III.4.3.3 The knowledge base 41
III.4.4 Fuzzy inference mechanism 41
III.4.5 The fuzzy systems advantages and disadvantages 42
III.4.6 The ANFIS Model 42
III.4.7 Hybrid learning algorithm 43
III.4.8 ANFIS advantages 44
III.5 Conclusion 44

CHAPTER IV: CRACK CHARACTERIZATION USING MACHINE LEARNING METHODS

IV.1 Introduction 46
IV.2 Calculation of the eddy current probe impedance 47
IV.3 Artificial neural networks 48
IV.3.1 Implementation of the artificial neural network 48
a. The choice of the neural network type 48
b. The choice of the learning strategy 49
c. The choice of the cost function 49
IV.3.2 Development of the learning database 50
IV.3.3 Crack detection for different length using the finite element results 51
IV.3.4 Evaluation of the crack lengths by artificial neural network PML 51
IV.3.4.1 Validation of results 53

IV.3.5 Crack detection for different depth using the finite elements results........................ 53

IV.3.6 Evaluation of the crack depths by artificial neural network PML 54

IV.3.7 Optimization of the neural network topology 55

IV.4 Deep learning method 57

IV.4.1 Implementation of the deep neural network... 58

IV.4.1.1 Module for deep learning... 58

IV.4.1.2 Topology optimization by unsupervised criteria 58

IV.4.2 Evaluation of the crack lengths by deep network.. 59

IV.4.2.1 Validation of results.. 59

IV.4.3 Evaluation of the crack depths by deep network... 60

IV.5 Hybrid machine learning method.. 61

IV.5.1 ANFIS architecture... 62

IV.5.2 ANFIS learning 62

IV.5.3 Evaluation of the crack lengths by Neuro-Fuzzy system (ANFIS)........................... 63

IV.5.3.1 Validation of results.. 64

IV.5.4 Evaluation of the crack depths by Neuro-Fuzzy System (ANFIS) 65

IV.6 Conclusion 65

General conclusion and perspectives……………………………………………………........67

Bibliographical references... 68

List of figures

Figure I.1- Generation of eddy currents in a conductive material [RAM 09] 2
Figure I.2- Measurement of impedance variation 3
Figure I.3- dual-function sensor 4
Figure I.4- separate function sensor 4
Figure I.5- Distribution of eddy currents in a flat surface 6
Figure I.6 - Influence of conductivity and lift-off on the normalized impedance diagram........ 8
Figure I.7- Sensor-crack device[HEL12] 8
Figure I.8 - Domain study 9
Figure I.9 - Interface between two media 11
Figure I.10 - Crack signature 16
Figure II. 1 - Impedance diagram 18
Figure II.2 - HF2LI device of Zurich Instruments 19
Figure II.3 - Schematic of measuring the amplitude and the phase of a signal relative to a defined reference signal, even if the signal is entirely buried in noise using Lock-in amplifier 20
Figure II.4 - Sensor impedance measurement circuit 21
Figure II.5 - Principle of sparking: 1 = piece, 2 = electrode, 3 = bath, 4 = resistance, 5 = capacitor, 6 = spark 23
Figure II.6 - Realized Stallion 24
Figure II.7 - Example of one of the cracks 25
Figure III.1- Formal neuron 27
Figure III.2- Monolayer Network 29
Figure III.3- Geometric representation of the XOR problem 30
Figure III.4 - Multilayer network 30
Figure III.5 - Perceptron model network 31
Figure III.6 - Example of multilayer perceptron 31
Figure III.7 - General diagram of supervised learning in neural networks 32
Figure III.8 - General diagram of unsupervised learning in neuranl networks 32
Figure III.9 - Illustration of the learning speed effect of a neural network: a) slow convergence of the algorithm when the speed is low, b) divergence of the algorithm due to a learning speed too large 34
Figure III.10 - Deep learning architecture 35
Figure III.11 - Schematic structure of an autoencoder with 3 fully connected hidden layers . 36
Figure III.12 - The fuzzy neural system 38
Figure III.13 - The membership function of a fuzzy set 39
Figure III.14 - Triangular membership function 40
Figure III.15 - Trapezoidal membership function 40
Figure III.16 - Gaussian membership function 41

Figure III.17 - General architecture of ANFIS 42
Figure IV.1 - Direct and inverse problems 46
Figure IV.2- Feed-forward neural network 49
Figure IV.3- Resistance variation as a function of the probe position for different crack lengths of the same thickness (0.20 mm) and the same depth (2 mm) 50
Figure IV.4 - a) Resistance variation, b) reactance variation: as a function of the probe position for different crack lengths of the same thickness (0.20 mm) and the same depth (2mm) 51
Figure IV.5 - Implementation of the neural network using for the estimation of geometric parameters 52
Figure IV.6 - a) MSE on learning and validation bases, b) correlation between the desired output and the network output for the crack lengths 52
Figure IV.7 - Estimated lengths according to the real lengths of the crack 53
Figure IV.8 - a) Resistance variation, b) reactance variation: as a function of the probe position for different crack depths of the same thickness (0.20 mm) and the same length (7mm) 54
Figure IV.9 - a) MSE on learning and validation bases, b) correlation between the desired output and the network output for crack depths 55
Figure IV.10 - Estimated depths according to the real depths of the crack 55
Figure IV.11 - Implementation of the neural network for length and depth crack outputs 56
Figure IV.12 - a) MSE on learning and validation bases, b) correlation between the desired output and the network output for crack lengths and crack depths 56
Figure IV.13 - Estimated neural network output according to the real output for the crack lengths and crack depths respectively 57
Figure IV.14 - Neural network and deep neural network 58
Figure IV.15 - Correlation between the desired output and the deep network output for crack lengths 59
Figure IV.16 - a) Estimated lengths according to the real lengths of the crack, b) correlation between the desired output and the deep network output for crack lengths 60
Figure IV.17 - Correlation between the desired output and the deep network output for crack depths for learning base 61
Figure IV.18 - a) Estimated depths according to the real depths of the crack, b) correlation between the desired output and the deep network output for crack depths 61
Figure IV.19 - ANFIS architecture with two inputs, one output, and four rules 62
Figure IV. 20 - ANFIS architecture for the crack lengths evaluation 63
Figure IV.21 - Correlation between the desired output and the ANFIS output for crack lengths 64
Figure IV.22 - Estimated lengths according to the real lengths of the crack for the validation database 64

Figure IV.23 - a) Correlation between the desired output and the ANFIS output for the crack depths, b) estimated depths according to the real depths of the crack for the validation database 65

List of tables

Table II.1- Dimensional data of the cracks carried out 25

Table III.1- Type of activation function 29

GENERAL INTRODUCTION

General Introduction

Concerning the dangers arising from the cracking of metal structures: sheet metal, pipes…etc., in the industrial sector (aviation, automobile, nuclear power), a quality control is often required. At the production level, it is necessary to dimension the pieces at the most just while guaranteeing their availability and performance. During the exploitation of an industrial product, its maintenance in good working order requires a good knowledge of the evolution of the parts which constitute it. This knowledge implies in particular to achieve tests shall not affect the integrity of parts or minimizing product availability.

For example, in a nuclear reactor, the fuel sheath constitutes a decisive factor for the installation safety. In fact, most of the incidents in such installations are due to the cracking and breaking of these sheaths [HUR 06, HUR 10, HEL 06], And the consequences of these incidents are often expressed in terms of human or environmental safety. This justifies the growing importance of non destructive testing (NDT). The challenge here is also of an economic nature: the speed and reliability of the evaluation technique employed are crucial in order to reduce the maintenance cost and to optimize the lifetime of the installations.

The NDT methods are used either to evaluate characteristic quantities of the product (thickness, conductivity…etc.) or to detect and characterize defects. Among the most widely used methods are ultrasound and electromagnetic methods (magnetoscopy, eddy currents). The choice of a method depends on a large number of factors such as the nature of the materials constituting the structure to be controlled, the nature of the information sought (open or buried defect), the conditions of implementation… etc.

Non destructive eddy current testing (NDT-EC) is frequently used for the control of electrically conductive parts, such as the control of tubes (nuclear, petroleum industry). It is a method that is simple to implement, it is easy to create eddy currents in a conductive medium by means of a probe, and complex in terms of creating a good distribution of the eddy currents to have a 'signature sensor' as important.

The design and the development of NDT-EC processes have become possible thanks to the numerical modeling of electromagnetic systems. This modeling also helps to understand the electrical and magnetic phenomena involved. The majority of work dedicated to the crack modeling of the NDT by EC process the resolution of the forward problem. Few of them relate the resolution of the inverse problem [HEL 12], which aims to characterize or identify either the physical or geometrical properties of the part in question.

Our objective in this work is to invert the data obtained by the sensor, for characterizing the surface cracks present in critical parts of conductive materials. Using a machine learning, this by exploring the different methodologies proposed by this approach. This choice is motivated by the ability of artificial intelligence methods modeled nonlinear problems.

A direct model was developed and validated by comparison with data obtained from an experimental companion performed in the laboratory according to the reference [HEL 12]. This validation uses known coils and calibration parts having well identified cracks. The inverse model is developed and validated using different approaches of machine learning.

This brief is divided into four chapters.

Chapter I: The non destructive testing by eddy currents

The first chapter presents the basic notions of nondestructive testing used in the industrial sector, the different types of defects detected in NDT, and also the different types of sensors used in the eddy current testing. An illustration of the eddy currents generation in a conductive material placed in the vicinity of an alternating current excited by the inductive sensor will be presented. The main mathematical formulation that allows to model electromagnetic phenomena in a non destructive eddy current testing and the numerical methods for characterization are recalled.

Chapter II: Experimentation: Test bench

In the second chapter, we study the effect of geometric parameters such as depth, length of defect on the response of the sensor by an experimental validation for the different algorithms witch we will develop them in the third and fourth chapters, it is in this context that we are interested in the practical realization of a test bench, dedicated to the experimental measurements of sensor impedance. The type of sensor used for detection works in differential mode, since the latter has the advantage of detecting micro cracks.

Chapter III: Machine Learning approaches

The third chapter explains in detail the theoretical background of the machine learning methods, which are: artificial neural networks, deep learning and hybrid methods. We gave an overview of different topologies for ANN, and their implementation which depends primarily on the nature of the problem to be treated. Deep learning method which describes a category of algorithms that use a pipeline of neural networks to learn a hierarchy of features, typically for classification tasks, and hybrid method that combine the techniques based in fuzzy logic and neural networks to eliminate the difficulties and inherent limitations of each isolated paradigm.

Chapter IV: Crack characterization using machine learning methods

The fourth chapter is devoted to the characterization of cracks by inversion techniques. The three approaches detailed in the second chapter are used to characterize the crack by reconstructing its length and depth from a database developed using finite element method simulation results and validated by an experimental measurement. Good inversion results for each technique are demonstrated.

We will finish this study with a general conclusion and perspective regarding the reconstruction of defects.

CHAPTER I

THE NON DESTRUCTIVE TESTING BY EDDY CURRENTS

I.1 Introduction

Quality has become an essential element of competitiveness, making it imperative for companies to acquire the best structures, tools and behaviors to ensure their sustainability in today's competitive environment. Among the tools used, non destructive testing techniques play a predominant role.

Non Destructive Testing (NDT) is a set of methods that characterize the integrity of structures or materials without degrading them either during production, during use or in phase of maintenance. They are used to ensure the safety of installations, particularly in the nuclear, aerospace, railway.

A definition of non destructive testing closer to the industrial reality thus consists in saying that it’s a matter of "qualifying, without necessarily quantifying, the state of a product without altering its characteristics in relation to standards, the execution of this task requires a good knowledge of the investigative methods used, their limits and above all a perfect match between the detection power of each one and the criteria applied for the implementation [DUM 96].

I.2 Non destructive testing methods

Although, there has no clearly defined boundary for non destructive testing [HAL 91], traditionally, it is considered that the majors and established methods are: visual testing, liquid penetrant testing, magnetic particle testing, radiographic testing, ultrasonic testing, acoustic emission testing and eddy current testing, they have their efficiency and their limits. Further, a large number of even new and more specialized methods have been investigated, developed and found to have applications in particular fields, such as for example thermography. The NDT techniques used are diverse, the choice of a method depends on:

1. The part to be controlled (nature of the material, shape ...).
2. The type of control to be carried out (detection of defects, thickness measurement, …).
3. The conditions under which the control should be performed.

I.2.1 The various defects detected in NDT

A defect detected in a piece is physically, highlighting heterogeneity of matter, a local variation of physical or chemical property prejudicial to the good use of it. However, it is customary to classify defects into two main categories related to their location: surface defects, internal defects.

I.2.1.1 The surface defects

These defects are accessible to the observer directly but not always visible to the naked eye. Corresponds to the most technologically harmful defects, since they are creeks, punctures, cracks, generally capable of eventually causing the rupture of the part, in for example initiating fatigue cracks. In metal parts, the thickness of these cracks is often tiny in the order of a few μm and they can be harmful as soon as their depth exceeds a few tenths of millimeter, which implies the use for their detection of sensitive and non destructive methods such as eddy currents and ultrasound.

I.2.1.2 The internal defects

Are heterogeneities of natures, shapes, and dimensions extremely varied, localized in the volume of the body to be controlled. In the metal industries, these will be internal cracks, porosities, various inclusions that may affect the health of molded, forged, laminated, welded parts. Here visual inspection is generally excluded, and we therefore use either of the major NDT processes, such as radiography, ultrasonic sounding or techniques better suited to specific situations such as acoustic emission, holography, infrared imaging.

I.3 Non destructive testing by eddy current

Non destructive testing by eddy current (NDT-EC) is the most widely technique used for detecting defects and characterizing the physical or geometrical properties of electrically conductive materials, thanks to its simplicity and efficiency [HEL 12]. NDT-EC is generally used to quantify various surface defects, such as cracks and chemical heterogeneities, microstructural or mechanical. It is also used to measure the thickness of metallic or insulating coatings on conductive materials.

I.3.1 Eddy currents generation

Eddy currents are induced currents developed in a closed circuit inside a conductive object placed in a magnetic field that varies over time.

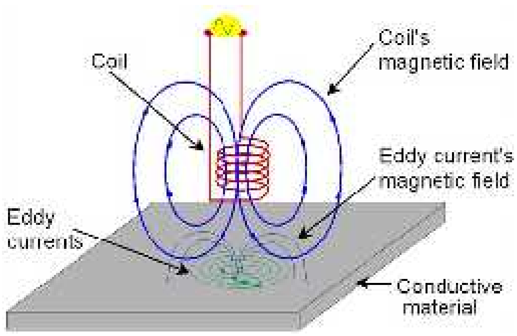

Figure I.1- Generation of eddy currents in a conductive material [RAM 09]

Examination by the eddy currents is based on the fact that if a coil is fed by a variable current and brought close to a conductive piece, generates such induced currents which themselves create a magnetic flux which, opposite to the generating flux, thus modify the impedance of this coil, it is the analysis of this impedance variation which will provide the exploitable information for a control. In fact, the path, the distribution and the intensity of the eddy currents depend on the physical and geometrical characteristics of the body under consideration, as excitation conditions (electrical and geometrical parameters of the winding).

It is therefore conceivable that a defect, constituting an electrical discontinuity disrupting the flow of the eddy currents, may give rise to a detectable impedance variation at the excitation coil [RAM 09]. Figure I.2 shows the process of eddy current inspection.

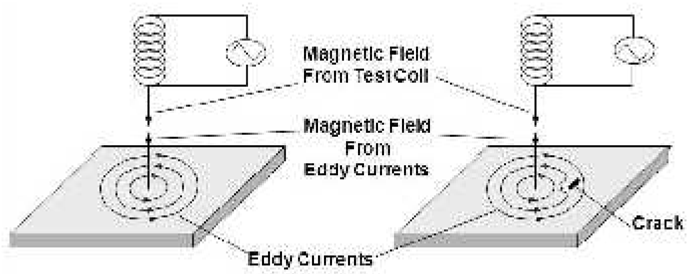

Figure I.2- Measurement of impedance variation

The defects are detected by variations in the impedance of the piece-coil system. This variation is of the order of 10^{-4} to 10^{-6} times the probe impedance [VUI 94].

I.3.2 Advantages and limits of eddy currents testing

a. Advantages

1. Simple, fast and inexpensive.
2. High sensitivity for defects detection.
3. No safety requirements for the operator or the environment.
4. Non-contact inspection.
5. Efficiency of the technique despite the complexity of the electromagnetic phenomena implemented.

b. Limits

1. The inspection depth depends on the excitation frequency.
2. Defects detection is a local way.
3. Inspection limited to electrically conductive materials.
4. The position of the sensor relative to the specimen could influence the detection efficiency of defects.
5. Competence and training are required for the personal inspection.

I.4 Different inductive Sensors

There are many ways to implement the winding to perform eddy current testing. Here we will list the basic configurations of the sensors.

I.4.1 Dual-function sensor

The dual-function sensor, it consists of a single transmitter-receiver coil that creates the alternating flow due to the current flowing through it and undergoes impedance variations that can be detected by very finely measuring of its output signal [DUM 96].

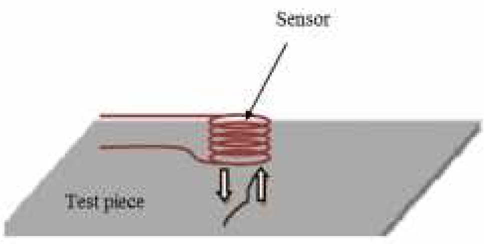

Figure I.3- dual-function sensor

I.4.2 Separate function sensor

The sensor with separate functions, it consists of two coils an exciter to create the flow and the other receiver to collect it. These two coils are molded in the same casing to avoid any accidental modification of their mutual.

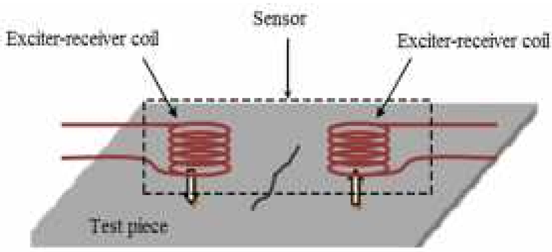

Figure I.4- separate function sensor

I.5 Operating mode

The measuring element can operate in absolute or differential mode

I.5.1 Absolute mode

Absolute mode allows access to all variables, whether useful or disturbing (e.g. temperature variation affects the conductivity σ and the permeability μ of the material to be controlled).

Absolute mode is generally well suited to the detection of long defects (extended corrosion, geometric defects with slowly variable dimensions such as variation in thickness, its main disadvantage remains the drift of the measurement in case of temperature variation [BOI 94].

I.5.2 Differential mode

A differential mode sensor is a probe intended to access only the local variations of the characteristics of the product under examination, by constant difference of two simultaneous measurements in two neighboring zones. The sensor can consist of two identical windings, the impedance variation of which is measured (Figure I-4). This probe is particularly used to detect discontinuities when moving along a piece [DUM 96].

I.6 Excitation mode in non destructive eddy current control

I.6.1 Mono-frequency excitation

During a mono-frequency test, the magnetic field is generated by a coil supplied with a sinusoidal current of fixed frequency. The choice of the frequency depends on the intended application and on the sensitivity to the desired parameters. The presence of a defect in a conductive part can be detected by measuring the impedance variation of the excitation coil for the breast sample compared to that measured over an area of the defective sample [BEN 06].

The use of a very low frequency generates very low amplitude of eddy currents and the precision becomes insufficient due to noise. On the other hand, the use of too high frequency gives rise to parasitic capacitive phenomena, generated in particular by the inter-turn capacities of the sensors [ZAO 08].

I.6.2 Multi-frequency excitation

Various methods of non destructive eddy current testing using several frequencies have been proposed to solve NDT problems. Multi-frequency data make it possible to obtain several useful information concerning the structure tested and thus to make the characterization more robust. For this type of NDT, the measurements at several frequencies are analyzed. To obtain them, the sensor is fed with a sinusoidal current successively at each of the frequencies under consideration. The data at each of these frequencies are collected as for mono-frequency measurements [BEN 06, ZAO 08, ZAI 12, BOU 14].

I.6.3 Pulse excitation

This method consists in emitting a magnetic field wide frequency band by exciting the sensor with a pulse signal (finite duration signal).

This mode of operation is commonly referred pulsed eddy current control. This technique was developed in the mid-1950s for the thickness measurement of metallic coatings [ZAI 12].

Work has also been carried out on its use for the detection of buried defects. The power supply signals may be rectangular, triangular or half-sine shaped. In this type of control, the temporal variation of the signals is used [BOU 14]. Given the spectrum of the excitation signal, such a method is richer in information than a control by mono-frequency or multi-frequency eddy currents. However, the amount of information collected in practice strongly depends on signal processing and noise which is difficult to filter because the signals are broadband.

I.7 Eddy currents penetration depth

In a plane conductor, the intensity of the eddy currents decreases with the depth below the surface according to an exponential law.

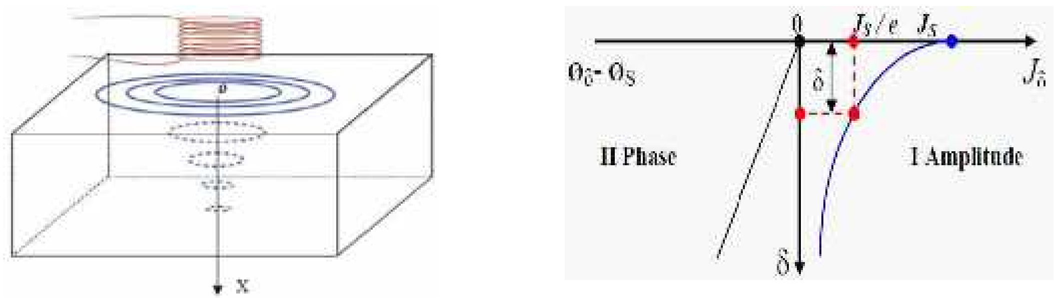

Figure I.5- Distribution of eddy currents in a flat surface

By convention, the depth of penetration δ in a conductor subjected to a uniform magnetic field $\vec{H}$ is the depth at which the intensity of the currents is equal to "$1/e$" or 37 % of the surface intensity, where e being the base of the natural logarithms ($e = 2.7183$) [GIL 88]. For a plane conductor, the depth of penetration δ is given by the following expression:

$$\delta = \frac{1}{\sqrt{\pi f \mu \sigma}} \tag{I.1}$$

Where

δ: Depth of penetration (m).

f: Frequency of the current through the coil (Hz).

μ: Magnetic permeability of the material (H/m).

σ: Electrical conductivity of the material (S/m).

This expression shows that:

- For a given material (μ and σ constants) the value of δ increases when the frequency f decreases and vice versa (skin effect).
- For a given frequency f, materials characterized by high magnetic permeability (ferromagnetic materials) or high electrical conductivity (copper, aluminum) have a low depth of penetration.

This phenomenon generates an exponential decay of the eddy current density, namely:

$$\delta J \ X = J_s e^{-X} \ \delta \tag{I.2}$$

I.8 Normalized impedance

The inductive sensor is always coil of N turns, of various shapes. It is characterized by two quantities: the resistive component (R) which includes the eddy current losses due to field penetration in the target and the internal losses of the excitation coil and the reactive term (X) represents the reactance of the excitation coil.

$$Z = R + jX \tag{I.3}$$

$$Z = \frac{V}{i_{exc}} \tag{I.4}$$

Where V and i_{exc} are the complex quantities associated to the voltage and the excitation current.

In order to keep the variations due to the presence of the piece in the expression of the impedance, the notion of normalized impedance is traditionally introduced [HEL 12]. This normalized impedance Z_n is deduced from Z using the expression:

$$Z_n = R_n + jX_n = \frac{Z - R_0}{X_0} \tag{I.5}$$

$$R_n = \frac{R - R_0}{X_0} \quad et \quad X_n = \frac{X}{X_0} \tag{I.6}$$

With $Z_0 = R_0 + X_0$ is the impedance of the vacuum sensor (without piece).

The measurement depends only on the structural parameters such as the excitation frequency and the geometry of the sensor and parameters of the piece to be controlled (its geometry, electrical conductivity σ, magnetic permeability μ) and its lift-off distance.

The study of the $Z_n$variations is carried out in the normalized impedances plane, by plotting X_n as a function of R_n. For a given sensor, any variation of one of the piece parameters induces a displacement of the representative point of Z_n in the normalized impedances plane.

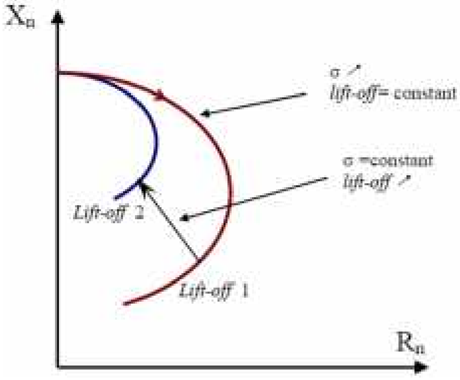

Figure I.6 - Influence of conductivity and lift-off on the normalized impedance diagram

Figure I-6 illustrates the shape of trajectories described by the probe impedance point for variations in electrical conductivity σ and piece-sensor distance [ABD 06, CHO 09].

I.9 Problematic of a NDT-EC system

The object of solving the NDT-EC problem is the complete characterization of the crack. A crack is defined by its morphology: position, shape, dimensions. The characterization of this crack passes by the determination of all these quantities. A control device may be presented by a block diagram (figure I-7) consisting of a coil placed above a conductive piece.

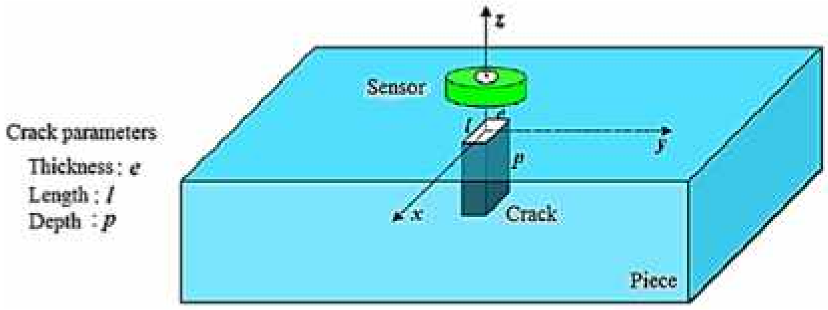

Figure I.7- Sensor-crack device[HEL12]

The development of non destructive testing systems requires the resolution of two problems: the direct problem and the inverse problem.

I.9.1 Direct problem

The direct problem is to determine the electromagnetic phenomena associated with the EC source, the sensor geometry and the piece considered. The electromagnetic phenomena involved in eddy current sensors are generally complex to model, but techniques have been proposed to achieve this. They are usually modeled numerically for example by the finite element method, or with semi-analytical methods [JOZ 06].

I.9.2 Inverse problem

The inverse problem makes it possible to estimate the useful parameters of the piece from the measured signals. It consists in estimating the electrical conductivity or the magnetic permeability of the analyzed material, or the geometry and the dimensions of the defect, on the magnetic field measurements generated by a given source. The inverse problems in electromagnetic are nonlinear and generally badly posed [ADR 10]. They are therefore difficult to solve.

I.10 Modeling of the electromagnetic problem

It should be noted that the primary objective aimed at in NDT by EC is to solve the inverse problem of eddy currents data. Most methods use a direct model linking the geometric quantities representative of the defect and the impedance variation of the coil. The direct model is generally based on the resolution of Maxwell's equations.

The problems related to the calculation of eddy currents can be schematized by a typical model composed of air, conductive material and a current source (Figure I-8). These objects form the computing domain Ω of boundary Γ.

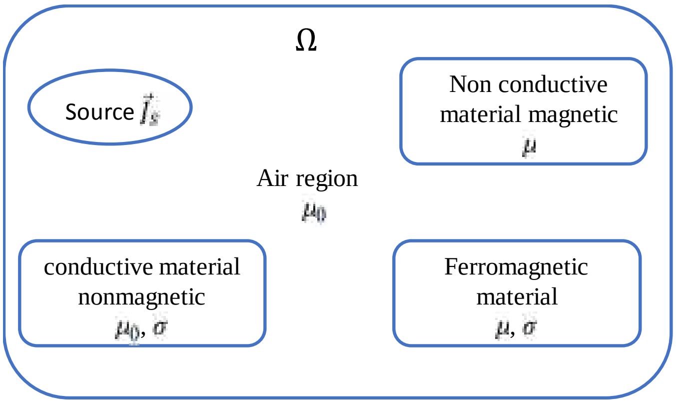

Figure I.8 - Domain study

I.10.1 Maxwell's equations

J. C. Maxwell (1831-1879) brought together all the electromagnetic phenomena into four equations called fundamental electromagnetism laws. Maxwell's equations constitute a system of partial differential equations which bind magnetic phenomena to electric phenomena:

1. Maxwell-Gauss equation

$$div\vec{D} = \rho \qquad \text{(I.7)}$$

2. Conservation equation of magnetic induction

$$div\vec{B} = 0 \qquad \text{(I.8)}$$

3. Maxwell-Faraday Equation

$$\overrightarrow{rot}\vec{E} = -\frac{\partial\vec{B}}{\partial t} \qquad \text{(I.9)}$$

4. Maxwell-Ampere equation

$$\overrightarrow{rot}\vec{H} = \vec{J}_t \qquad \text{(I.10)}$$

Where

$\vec{B}$: Magnetic induction (T).

$\vec{H}$: Magnetic field (A/m).

$\vec{D}$: Electrical induction (C/m^2).

$\vec{E}$: Electric field (V/m).

$\vec{J}_t$: Total current density (A/m^2).

ρ : Volume charge density (C/m^3).

Indeed, these equations constitute an incomplete equations system, we must add relations that describe the medium studied (the laws of behavior):

$$\vec{J} = \vec{J}_s + \sigma\vec{E} \qquad \text{(I.11)}$$

$$\vec{B} = \mu\vec{H} + \vec{B}_r \qquad \text{(I.12)}$$

$$\vec{D} = \varepsilon\vec{E} \qquad \text{(I.13)}$$

Where

$\vec{J}_s$: Current source density [A/m^2].

σ: Electrical conductivity [S/m].

μ: Magnetic permeability [H/m].

$\vec{B}_r$: Remnant magnetic induction [T].

ε: Electrical permittivity [F/m].

I.10.2 Continuity and boundary conditions

a. Continuity conditions

The electromagnetic fields undergo discontinuities when passing between two media of different properties. The transmission or passage conditions are then written at the interface between two media (Figure I-9).

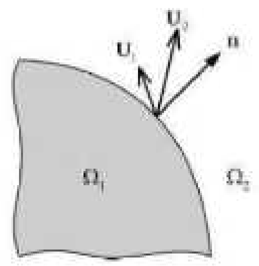

Figure I.9 - Interface between two media

$$(\vec{D}_2 - \vec{D}_1).\vec{n} = \rho_s \tag{I.14}$$

$$(\vec{B}_2 - \vec{B}_1).\vec{n} = 0 \tag{I.15}$$

$$(\vec{E}_2 - \vec{E}_1) \wedge \vec{n} = 0 \tag{I.16}$$

$$(\vec{H}_2 - \vec{H}_1) \wedge \vec{n} = \vec{J}_s \tag{I.17}$$

Where ρ_s is the surface density of charge, $\vec{J}_s$the surface density of current and $\vec{n}$ the vector normal to the separation surface of the two media Ω_1 and Ω_2 and directed towards the outside of the medium 1.

b. Boundary conditions

Generally, for a variable u, the boundary conditions are stated for a domain Ω of boundary Γ as follows:

- Dirichlet condition homogeneous: $u.\vec{n} = 0$.
- Neumann condition homogeneous: $\frac{\partial u}{\partial t} = 0$.

$\vec{n}$ is a normal vector to Γ.

I.11 Formulation of the magnetodynamic problem

A formulation is an association with constitutive relations, passing relations, boundary conditions and gauge conditions. The formulation is the choice of the unknown variables and their equation. It is often preferred to express the electric and magnetic fields as a function of potentials. Indeed [REN 99] has shown that the system obtained by taking as unknown fields $(\vec{E}, \vec{H})$ converges less well than if one works with potentials.

I.11.1 General formulation in potentials $(\vec{A}, V)$

Several formulations exist for solving electromagnetic problems such as the magnetic vector potential formulation, the electric field formulation $\vec{E}$, the formulation in $\vec{A}$ has been introduced by several authors such as, for example, in [KAN 03]…etc.

At the present time, the formulation which remains attractive for the problems resolution of the eddy currents calculation in 3D is that in potentials $\vec{A}$–V($\vec{A}$ is the magnetic vector potential and V is the electrical scalar potential).

In the following, we are interested in the formulation $\vec{A}$ -V in the general case. Rewrite the two Maxwell equations:

$$\overrightarrow{rot}\vec{E} = -\frac{\partial \vec{B}}{\partial t} \quad \text{(I.18)}$$

$$div\vec{B} = 0 \quad \text{(I.19)}$$

The second equation indicates that there exists a vector $\vec{A}$ given by:

$$\vec{B} = \overrightarrow{rot}\vec{A} \quad \text{(I.20)}$$

The vector $\vec{A}$ is called the magnetic vector potential. The substitution of (I.19) in (I.17) gives:

$$\overrightarrow{rot}(\vec{E} + \frac{\partial \vec{A}}{\partial t}) = 0 \quad \text{(I.21)}$$

This allows us to note that the field $\overrightarrow{rot}(\vec{E} + \frac{\partial \vec{A}}{\partial t})$ is a conservative field, it then comes:

$$(\vec{E} + \frac{\partial \vec{A}}{\partial t}) = -gradV \tag{I.22}$$

So:

$$\vec{E} = -\frac{\partial \vec{A}}{\partial t} - gradV \tag{I.23}$$

From equation (I.10) and equation (I.12) we have:

$$\overrightarrow{rot}\ \frac{1}{\mu}\vec{B} = \vec{J}_t \tag{I.24}$$

From the equations (I.11), (I.20) and (I.23) we have:

$$\overrightarrow{rot}(\frac{1}{\mu}\overrightarrow{rot}A) = -\sigma\ \frac{\partial \vec{A}}{\partial t} + gradV + \vec{J}_s \tag{I.25}$$

In order to solve this equation with two unknowns $(\vec{A}, V)$, we must fix the potential divergence $\vec{A}$ to ensure the uniqueness of the solution. We add the condition $div\vec{A} = 0$ called Coulomb gauge:

$$\begin{cases} \overrightarrow{rot}\ \frac{1}{\mu}\overrightarrow{rot}\vec{A} + \sigma\ \frac{\partial \vec{A}}{\partial t} + gradv = \vec{J}_s \\ div\vec{A} = 0 \end{cases} \tag{I.26}$$

I.11.2 Numerical methods of discretization

The phenomena that describe the behavior of electromagnetic devices are represented by partial differential equations. In general, these equations are solved using analytical methods or numerical methods. For more complex geometries, numerical methods have been used which use discretization techniques. Indeed, they transform partial differential equations of the field in a system of algebraic equations taking into account the boundary conditions.

The solution provides an approximation of the unknown at different points located at the nodes of the geometric network corresponding to the discretization. The main numerical methods are: The finite difference method (FDM), the finite element method (FEM), the boundary integral method (BIM) and the finite volume method (FVM) [BEL 03].

I.11.2.1 Finite difference method (FDM)

The finite difference method is relatively simple to implement but has the disadvantage of having a poor approximation quality of the variables and the inability to model complex shape geometries.

The method is based on Taylor's theorem which we replace the differential operator by operator differences. The domain of study is divided by means of a square grid in the two-dimensional case and a cubic grid in the three-dimensional case, the equation to be solved is written for each node of the mesh. The method is difficult to apply to domains with complex geometry, but is reserved for domains with simple geometry and regular boundaries such as squares and rectangles [BEL 03, KHE 06].

I.11.2.2 Finite element method (FEM)

Without doubt, the finite elements occupy a large place in the modeling. Unlike FDM, finite elements adapt well to complex geometries, they can greatly improve the calculation accuracy by taking into account different types of interpolation functions of variables. The method consists in meshing the space into elementary regions in which the desired quantity is represented by a polynomial approximation. The mesh can be made up of triangles or rectangles in 2D case and tetrahedron or parallelepiped in 3D case with peaks which are searched for values of the unknown. The method leads to large algebraic systems, and therefore requires a large memory of calculator.

The advantage of adapting to complex geometries and taking account of non-linearities has made the finite element method widely used in electromagnetism although it is a little difficult to implement since it requires a large capacity of memory and a large calculation time [BEL 03, KHE 06].

I.11.2.3 Boundary integral method (BIM)

When using FDM or FEM, unknown variables are calculated throughout the domain. The BIM allows to reduce the mesh to the domain boundary, the calculation of the unknown values on the boundaries of the domain is sufficient to obtain the solution at any point of the domain. To reduce the problem of borders, the BIM uses the Ostrogradski-Green theorem. This method may be of interest for the study of three-dimensional structures where air or passive environments occupy much the study domain.

However, this method has the disadvantage of leading to a full matrix algebraic system with no null terms. This increases the user time, so the calculation cost [BEL 03, KHE 06].

I.11.2.4 Finite volume method (FVM)

The finite volume method is a discretization method used especially in fluid mechanics. The method of finite volumes has grown considerably not only for modeling in fluid mechanics, but also for the modeling of other branches of engineering: thermal transfer, electromagnetism ... etc. The method consists in subdividing the domain of study into elementary volumes (tetrahedrons, hexahedrons, prisms, etc.) in such a way that each volume surrounds a node.

The PDE equation of the problem is integrated on an elementary volume. In order to calculate the integral on this elementary volume, the unknown is represented by an approximation function between two consecutive nodes. Then, the integral form is discretized in the domain of study [BEL 03, KHE 06]. Compared to finite elements, the discretization by finite volume method leads to a linear system with a sparse matrix. This advantage allows faster convergence of iterative solvers [CHE 07].

I.11.3 Calculation of the impedance variation

The impedance variation can be determined by calculating the stored magnetic energy W_m in the entire study space and the Joule losses P_J defined by the following expressions:

$$W_m = \frac{1}{2} \quad \frac{1}{\mu} \vec{B}^{\,2} dv \qquad \text{(I.28)}$$

$$P_J = \frac{1}{2} \quad \frac{1}{\sigma} \vec{J}^{\,2} dv \qquad \text{(I.29)}$$

With $\vec{B}$: Magnetic induction [T].

μ: Magnetic permeability [H/m].

$\vec{J}$: Density of eddy currents [A/m^2].

σ: Electrical conductivity [S/m].

Knowing W_m and P_J, we can easily trace the equivalent resistance R and the reactance X of the sensor. The expressions relating the resistance to the Joule losses and the reactance to the magnetic energy are given by the following relations [IDA 88, HEL 12]:

$$P_J = RI^2 \qquad \text{(I.30)}$$

$$W_m = \frac{1}{2\omega} X I^2 \qquad \text{(I.31)}$$

With I and ω represent respectively the excitation current through the coil and its pulsation.

The measurement of these quantities must be made for a material without defects and for a material having defects. The impedance of the probe is called Z and it variation ΔZ.

I.11.4 Representation of eddy current signals

We perform position changes of the sensor at a low pitch of $1\ mm$ along the half surface of a piece containing crack. We first calculate the magnetic vector potential and electric scalar in each position, then we deduce the impedance variation by using equations (I.30) and (I.31).

Are presented in figure I-10 the eddy current signals, namely the variations of the resistance and reactance of the sensor, recorded on the Aluminum plate containing a straight slot (perpendicular to the sample surface) of $2\ mm$ deep, $1\ mm$ long and $0.20\ mm$ thick. These signals constitute the signature of the slot.

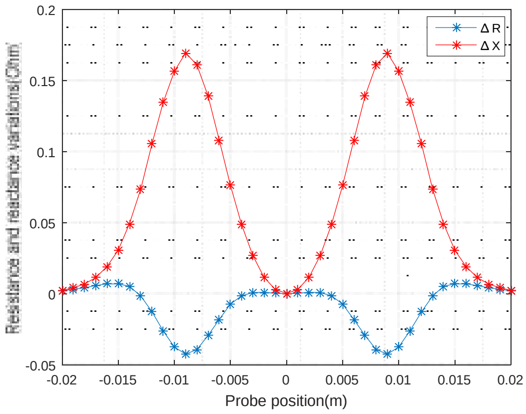

Figure I.10 - Crack signature

I.12 Conclusion

In this chapter, we briefly recalled the definition and the purpose of non destructive testing (NDT), the different types of defects detected in NDT. It is the nondestructive testing by eddy currents (NDT-EC) which constitutes the subject of this work, the choice of this testing is justified by its simplicity, inexpensive practical realization and its efficiency. We reported notions on the creation of eddy currents, also the basic notions about the inductive sensors used in this non destructive testing, the advantages and limitations of this method.

In the second part, we have presented the formulation relative to the magnetodynamic problem. As well as the presentation of some numerical methods of discretization FDM, FEM, BIM and FVM which transform partial differential equations in systems of algebraic equation.

The signals representing the resistance and the reactance variations as a function of the sensor position were adopted as characteristic signatures of the modeled crack were also presented.

CHAPTER II

EXPERIMENTATION:

TEST BENCH

II.1 Introduction

The eddy current technique is one of the most used for fast inspection of conductive parts, tubes ... etc. The presence of a defect modifies the trajectory of the induced currents and alters the magnetic flux whose amplitude and distribution depends on the position and shape of the defect. Non destructive testing is an advanced discipline that is necessary for the detection and evaluation of geometric and physical characteristics in the structure of a material using eddy current sensors. These sensors can work in absolute or differential mode to detect a wide variety of defects [DID 92]. The majority of the scientific work in the literature considering the non destructive control by eddy currents treats the detection of defect appearing in the materials like loss of material (fissure, vacuole ...) [RAV 08]. However, other defects can appear without loss of matter [BOU 13, BEN 14]. Exemplary Mention: small inclusions, small burns and micro welds.

In this chapter, we study the effect of geometric parameters such as depth, length of defect on the response of the sensor and make an experimental validation for the different algorithms witch will develop them in the third and fourth chapters, it is in this context that we are interested in the practical realization of a test bench, dedicated to the experimental measurements of sensor impedance. The type of sensor used for detection works in differential mode, since the latter has the advantage of detecting micro cracks.

II.2 Impedance Diagram

As detailed in the first chapter, the inspection of materials consists of measuring the impedance variations of the coil. In general, a comparative method is used, the purpose of which is to measure the difference between the impedance Z of the coil in the presence of the part to be inspected and the impedance Z_0 of the coil in the area (in the absence of the material to be controlled), the complex impedance Z_0 of the sensor is given by [SHU 02]:

$$Z_0 = R_0 + jX_0 \tag{II.1}$$

R_0 and X_0 are respectively the no-load resistance and reactance of the sensor.

In the presence of the material to be controlled. The complex impedance in charge is:

$$Z = R + jX \tag{II.2}$$

To eliminate the components of the vacuum impedance R_0 and X0 (no-load losses, sensor's own inductance) and to keep only the geometry of the sensor, its relative position to the material (lift-off) and the geometrical and physical characteristics of the material, Performs the normalization of the complex impedance of the sensor in the presence of the material, this normalization is given by:

$$Z_n = R_n + jX_n = \frac{Z - R_0}{X_0} \tag{II.3}$$

$$R_n = \frac{R - R_0}{X_0} \quad et \quad X_n = \frac{X}{X_0} \tag{II.4}$$

The impedance of the coil can be represented in the impedance plane whose horizontal axis represents the real part and the vertical axis the imaginary part, figure II.1. A vacuum (i.e. when the coil is sufficiently far from the material), the coil impedance is represented by $Z_0\ (R_0, X_0)$, located at point 1. In the presence of a conductive target and due to the influence of the magnetic field created by the eddy currents that opposes the excitation field, the coil impedance varies in relation to Z_0 and is presented by $Z_1(R_1, X_1)$, at the point 2 [BEN 06], and if the inspected conductive target includes a defect, the impedance is shown at point 3 corresponding to the defect center.

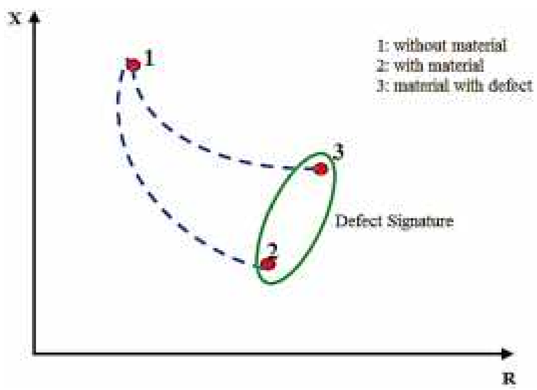

Figure II. 1 - Impedance diagram

For a given coil, and for a fixed frequency, $Z1$ is a function of the electrical, magnetic and geometrical properties of the conductive material part situated in the zone influenced by the magnetic field of the coil. Any variation of these parameters will cause a displacement of Z_1 in the impedance plane. By this phenomenon, it is possible to detect a variation in the conductivity or a variation in the dimensions of the material [BOU 14].

II.3 Sensor impedance measuring equipment

Our choice was directed to a lock-in amplifier instrument, which serves for non destructive eddy currents testing and can allows Fresnel representation (electronically) of a signal by measuring its amplitude and its phase with respect to a reference signal.

Lock-in amplifiers were invented in the 1930’s [COS 34, MIC 38, MIC 41] and commercialized in the mid-20th century as electrical instruments capable of extracting signal amplitudes and phases in extremely noisy environments. They employ a homodyne detection scheme and low-pass filtering to measure a signal’s amplitude and phase relative to a periodic reference.

A lock-in measurement extracts signals in a defined frequency band around the reference frequency, efficiently rejecting all other frequency components. The best instruments on the market today have a dynamic reserve of 120 dB [web page], which means they are capable of accurately measuring a signal in the presence of noise up to a million times higher in amplitude than the signal of interest.

Lock-in amplifiers are extremely versatile. As essential as spectrum analyzers and oscilloscopes, they are workhorses in all kinds of laboratory setups, from physics to engineering and life sciences. As with most powerful tools, only a solid understanding of the working principles and features enables the user to get the most out of it and to successfully design experiments.

The HF2LI amplifier, shown in Figure II.2, manufactured by Zurich Instrument, is a voltage measuring device based on the lock-in amplifier principle.

Figure II.2 - HF2LI device of Zurich Instruments

The front panel of the BNC connectors and the control LEDs are organized in 5 sections, from left to right, the two pairs of single ended and differential inputs (1 and 2). The two output blocks each with an add input, analog and a synchronization output, as well as auxiliary outputs.

The main features of this device are:

1. Analogue signal measurement range from 0.7 μHz to 50 MHz.
2. Ability to generate and measure up to 6 signals of different frequencies simultaneously.
3. Two outputs and two single ended / differential inputs 50Ω / 1MΩ each can be used independently in single or differential measurement.
4. Generation of output signals with 16-bit resolution for ± 10 mV, ± 100 mV, ± 1 V or ± 10 V ranges.

This is more of a digital device, all functions whose signal generation and filtering are performed by logic functions. The device is controlled from a computer software via the USB port, which allows the setting of good numbers of parameters including signal frequencies, their amplitudes, and the properties of the filters.

II.3.1 Lock-in amplifier HF2LI working principle

A lock-in amplifier performs a multiplication of its input with a reference signal (Figure II.3), also sometimes called down-mixing or homodyne detection, and then applies an adjustable low-pass filter to the result. This method is termed demodulation and isolates the signal at the frequency of interest from all other frequency components.

The reference signal is either generated by the lock-in amplifier itself or provided to the lock-in amplifier and the experiment by an external source. The reference signal is usually a sine wave but could have other forms, too.

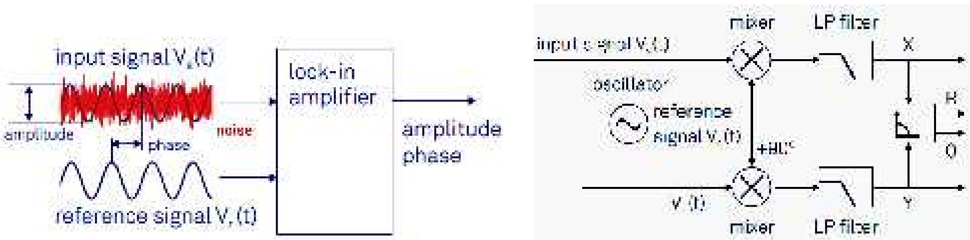

Figure II.3 - Schematic of measuring the amplitude and the phase of a signal relative to a defined reference signal, even if the signal is entirely buried in noise using Lock-in amplifier

The device response $V_s(t)$ as well as the reference signal $V_r(t)$ are used by the lock-in amplifier to determine the amplitude R and phase Θ. This is achieved using a so-called dual-phase demodulation circuit, as illustrated in figure II.3. The input signal is split and separately multiplied with the reference signal and a 90◦ phase-shifted copy of it.

The dual-phase down-mixing is mathematically expressed as a multiplication of the input signal with the complex reference signal, where:

$$V_s(t) = a.\cos(\omega_s t + \theta) = \frac{a}{2}\ e^{i(\omega_s t+\theta)} + e^{-i(\omega_s t+\theta)}] \qquad \text{(II.5)}$$

$$V_r(t) = be^{-i\omega_r t} = b.cos(\omega_r t) - i.b.sin(\omega_r t) \qquad \text{(II.6)}$$

V_s and V_r are respectively, the input signal and reference signal.

The complex signal after mixing is given by:

$$V_{out}(t) = X(t) + iY(t) = R\ e^{i[(\omega_s-\omega_r)t+\theta]} + e^{-i[(\omega_s+\omega_r)t+\theta]}] \qquad \text{(II.7)}$$

It comes due to the trigonometric identity:

$$\sin(a)\sin(b) = \frac{1}{2}[\cos(a-b) - \cos(a+b)] \qquad \text{(II.8)}$$

The filtering operation eliminate the component $e^{-i[(\omega_S+\omega_r)t+\theta]} = 0$. The averaged signal after demodulation becomes:

$$V_{out}(t) = Re^{i[(\omega_S-\omega_r)t+\theta]} \qquad \text{(II.9)}$$

In the case of equal frequencies $\omega_s = \omega_r$, this further simplifies to:

$$V_{out}(t) = Re^{i\theta} \qquad \text{(II.10)}$$

The outputs of the mixers (figure II.3), pass through configurable low-pass filters, resulting in the two outputs X and Y, termed the in-phase and quadrature component. The amplitude R and the phase Θ are easily derived from X and Y by a transformation from Cartesian coordinates into polar coordinates using the relation:

$$R = \sqrt{X^2 + Y^2} \quad and \quad \theta = \text{atan}(Y, X) \qquad \text{(II.11)}$$

II.3.2 Sensor Impedance Measurement

In order to characterize the evolution of the sensor impedance in the complex impedance plane, we have made a test bench which is shown schematically in figure II.4.

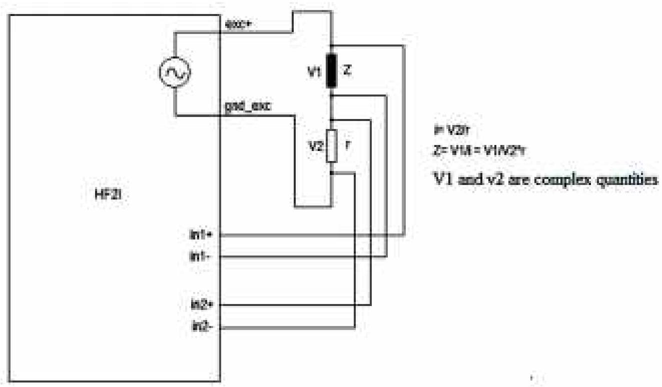

Figure II.4 - Sensor impedance measurement circuit

The sensor representing the load Z is excited by an internal voltage source of lock-in amplifier HF2LI from a few kHz to a few tens MHz. This sensor is connected in series with a resistor of low value (r = 10 Ohm). The value of the resistance being much greater than the impedance of the sensor, it allows to fix the value of the current flowing in the sensor. The current flowing through the sensor was set at 0.1 A rms (generator voltage 1 V rms).

The measured voltage across the sensor via synchronous detection and the current flowing through the sensor allow us to determine the impedance of the sensor. It can be simplified by a multiplier and a low pass filter, by multiplying the signal at the output of the sensor by a reference signal of the same frequency f a continuous part and a frequency $2f$ part are obtained. By using a low pass filter, we then keep the continuous part which corresponds to the module part of the signal.

II.4 Materials to be inspected

Over the years, sensor technology and data processing have continuously progressed and today the eddy current technique is known to be fast, simple and accurate. This is why it is widely used in the production and use of metal products for surface and volume detection and the physical characterization of materials such as Aluminum, Stainless Steel, Copper, Titanium, Brass and even carbon steel. The material to be inspected is the seat of the eddy currents.

II.4.1 Calibration parts qualities

The stallions of measures have a very important role in the quality of the measurement and results. The eddy current testing method is based on the reproducibility of results compared to a calibration. It is important to know perfectly the qualities to be required of a calibration piece

1. Parts of simple geometry: wires, tubes, bars, plates ... etc.
2. To determine a standard part, it is necessary to have an identical batch of the same quality and size.
3. Before performing the standard defects, these parts are controlled by eddy current to eliminate those which will present a visual non-detectable anomaly.
4. Calibration defects to achieve should be close to actual defects to be detected
    - A hole is similar to a crevice.
    - A thickness reduction is similar to extensive corrosion.
    - A slot may be a crack.
5. These defects must be carried out without tracing or pointing.

Using a set of calibrated defects introduced on the material. We chose to work with materials of different shades and different electrical and magnetic characteristics. We chose the following materials:

- A ferromagnetic soft steel, in this case the XC38 steel, chosen because of its current use in mechanical engineering [HEL 06].
- A non-magnetic austenitic stainless steel, in this case AISI 304 steel. This material has been chosen for its important use in various fields, including nuclear engineering thanks to its resistance to corrosion under severe operating conditions [DEP 03].

The detection sensitivity of a control process is generally based on the nature and dimensions of the smallest detectable defect.

At the present time, "defects" which simulate as much as possible real defects are artificially realized by drilling, milling, electrical discharge machining, ultrasonic machining or laser beam, diffusion welding [DEP 03].

II.4.2 Electrical discharge machining

Electrical discharge machining (EDM), is a machining process which involves removing material in a piece using electric discharges. We also talk about spark machining. This technique is characterized by its ability to machine all electrically conducting materials (metals, alloys, carbides, graphites, etc.) whatever their hardness. There are three types of EDM:

1. Electrical discharge machining by sinking in which an electrode of shape complementary to the shape to be machined sinks into the part.
2. Electrical discharge machining by wire, where an animated conductive wire with a planar and angular motion cuts a part along a set surface.
3. The speed drilling using a tubular electrode for drilling very hard materials.

To machine by sinking EDM, four elements are required:

An electrode, a piece, a dielectric (electrically insulating liquid), and electricity.

II.4.2.1 EDM principle

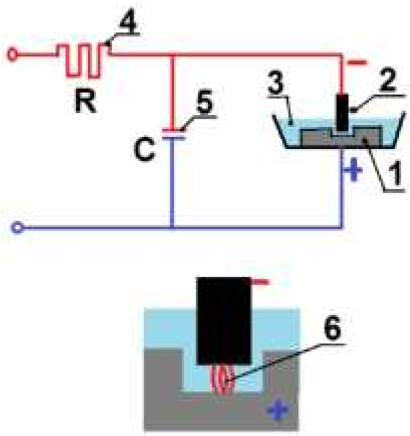

Figure II.5 - Principle of sparking: 1 = piece, 2 = electrode, 3 = bath,

4 = resistance, 5 = capacitor, 6 = spark

The principle of the EDM is simple. The workpiece and tool are positioned so that they are not in contact. There remains a space which is then filled with insulating liquid. This is why the treatment is carried out in a container. Piece and tool are connected by a cable to a direct current source. On an electric wire, there is a switch, if the latter is closed, an electrical voltage is then formed between the workpiece and the tool.

Firstly, no current flows because the dielectric fluid between the workpiece and the tool acts as an insulator. However, if space is reduced, a spark gushes when the distance is very small. During this reaction, called discharge, the current is transformed into heat, the surface of the material heats up strongly in the region of the discharge channel. If the current supply is interrupted, the discharge channel is quickly canceled out. The molten metal on the surface of the material then evaporates in an explosion and removes the liquid material to a certain depth. A small crater forms, if the discharges succeed, craters appear side by side and there is therefore a constant erosion on the piece surface.

II.4.2.2 Opportunities and benefits

- Machining and drilling of hard metals: carbides.
- Very good precision and good surface condition.
- machining of special shapes (square holes, triangular, helical, complex engravings).

II.4.3 Stallions

Crack defects are frequently encountered in NDT, their geometry is characterized by the fact that one of the dimensions is very small compared to the other two [BIH 08], it is this type of defect that we will consider in this chapter.

Parallelepiped cracks with different depths and lengths simulating open cracks were performed by EDM on XC38, AISI 304 samples by the Central Logistics Base (CLB-Algiers) (Figure II.6).

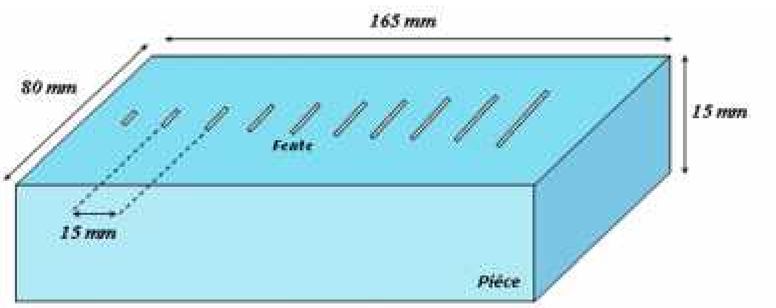

Figure II.6 - Realized Stallion

Crack	Length *l*(mm)	Depth *p*(mm)	Thickness *e*(mm)
1	1	1	
2	2	2	
3	3	3	
4	4	4	
5	5	5	The thinnest possible for this thickness
6	6	6	
7	7	7	
8	8	8	
9	9	9	
10	10	10	

Table II.1- Dimensional data of the cracks carried out

An example of one of the cracks is given in the figure II.7.

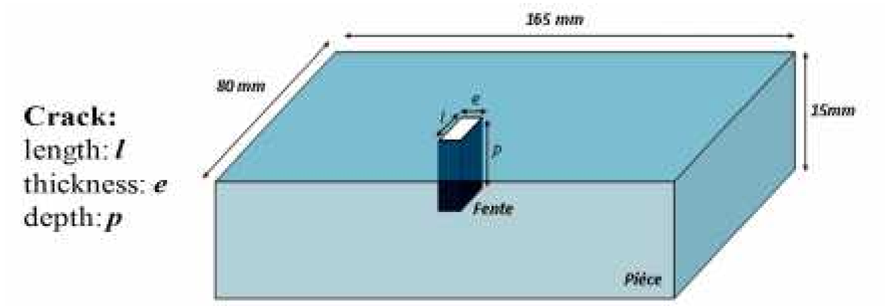

Figure II.7 - Example of one of the cracks

II.4.4 Sensor position relative to the sample

The defect signal amplitude depends on the ratio (defect volume / examined volume), it is therefore a function of the dimension of the sensor. The best detection is obtained when the eddy currents are perpendicular to the defect.

The increase in the sensor dimensions improves the area of surface examined, whereas the sensitivity is reduced. The distance of the sensor from the sample to be controlled decreases the sensitivity.

II.5 Measurement steps

Synchronous detection makes it possible to extract the module and the phase of the measurement signal, in other words, it makes it possible to supply the reactive and active components of the measurement signal (abscissa and ordinate resulting from the phase and quadrature demodulation respectively of the measuring signal) [SHA 97].

The main functions of an eddy current instrument are:

II.5.1 Excitation

There are two types of generator:

1. Single-frequency generator, providing one or a few switchable fixed frequencies, or even a continuously variable frequency: it allows to carry out tests just one frequency at a time.
2. Multi-frequency generator, providing simultaneously two to four fixed or variable frequencies (continuous tuning): it allows to carry out tests at several frequencies at the same time using the same probe.

II.5.2 Modulation and filtering

The modulation is created by the presence of the object to be controlled in the vicinity of the winding. In order to improve the signal-to-noise ratio, compensation and amplification of the signal is provided by the filtering operation.

II.5.3 Demodulation and visualization of the signal

This is the most important operation in a measuring chain: it consists of a synchronous detection which makes it possible to extract the module and the phase of the measurement signal. The visualization consists of visualizing the measurement signal on the screen of an oscilloscope or a computer.

CHAPTER III

MACHINE LEARNING APPROACHES

III.1 Introduction

Machine learning is a field of artificial intelligence study. It concerns the design, analysis, development and implementation of methods allowing a machine to evolve through a systematic process, Tasks or problems difficult to fulfill by more conventional algorithmic means. The algorithms make it possible, for a system controlled by a computer, to adapt its analyzes and behaviors in response, based on the analysis of empirical data from a database or sensors.

Machine learning uses the theory of statistics because the main task is to make an inference from a sample. In this case, the role of computing is twofold: first, in learning, we need efficient algorithms to solve the optimization problem, as well as to store and process the massive amount of data we generally have, Secondly, once a model is learned; its representation and its algorithmic solution for inference must be as effective.

In this part, we will describe different approaches, which will be used later to solve the inverse problem.

III.2 Artificial neural networks

The brain able to learn and perform complex reasoning consists of a very large number of neurons (about 10^{15}) interconnected (10^3 to 10^4 connections per neuron). Artificial neural networks are one of the artificial intelligence approaches that have been developed for primary objective the modeling and understanding of brain function.

Neural networks are sets of basic elements called neurons. The philosophy behind these neural networks is to imitate the human brain, but the gap between neural networks and the brain is always large, due to the complexity of the last.

III.2.1 Formal Neuron

The formal neuron is described as an elementary processor, with an activation function f also called a transfer or decision function, which receives a number n of p input variables from upstream neurons. Each of these inputs is weighted by a weight w_n which represents the strength of the connection.

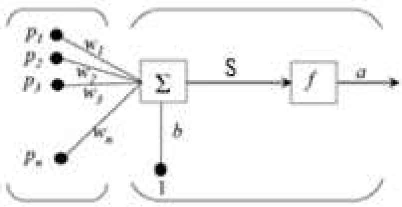

$$a = f(\sum w_i p_i + b)$$

Figure III.1- Formal neuron

The scalars of inputs p_i are multiplied by the weight scalars w_i to form $w_i * p_i$, one of the terms of the sum. The other input, initiated at 1, is multiplied by the bias b, and then introduced into the sum. The output sum S, often referred to as the network input, passes into the transfer function f which produces the output scalar a.

If we relate this simple model to the biological neuron, the weight w corresponds to the strength of the synapse, the cell is represented by the sum, the transfer function and the output neuron corresponds to the axon signal, the output neuron is calculated by the equation:

$$a = f \sum w_i p_i + b \tag{III.1}$$

Typically, the transfer function f is selected by the user and the w and b parameters are adjusted by learning laws so as to adapt the neuron for a specific purpose.

III.2.2 Transfer functions

This function can be linear or not, it allows to define the internal state of the neuron. A particular function is chosen to satisfy the specificities of a problem that the neural network is expected to solve. These include for example, three main types of the most popular functions: binary threshold, ramp with saturation, and sigmoid.

a. Binary threshold function

The activation function that was used in [UTK 93]. The threshold introduces a non-linearity in the behavior of the neuron, it is the all-or-nothing model.

b. Ramp function with saturation

This function represents a compromise between the linear function and the threshold function, between its two terminals; it gives the neuron a linear combination of the input. At the limit, the linear function is equivalent to the threshold function.

c. Sigmoid function

The sigmoid function is a continuous function which maintains the output in the interval [0,1]. Its main advantage is the existence of its derivative at any point. It is generally used in the multilayer perceptron [OZD 89].

Table III.1 summarizes these three main types of activation function.

Type of function	***Curves***	***Equations***
Binary threshold function	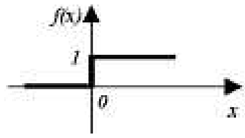	$f(x) = \begin{cases} 1 & if\ x > 0 \\ 0 & otherwise \end{cases}$
Ramp function with saturation	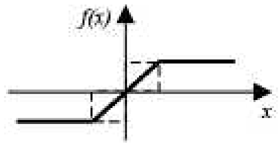	$f(x) = \begin{cases} x & if\ x \in [u, v] \\ v & if\ x \geq v \\ u & if\ x \leq u \end{cases}$
Sigmoid function	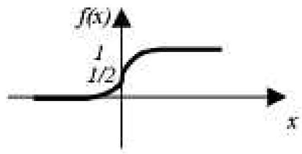	$f(x) = \dfrac{1}{1 + e^{-x}}$

Table III.1- Type of activation function

III.2.3 Network architecture

The connections between the neurons composing the network describe the topology of the model, which may be diverse, but among the most commonly used, we distinguish:

III.2.3.1 Feedforward neural networks

For this type of network, the neurons are grouped into layers. All neurons in one layer hold their inputs from the previous layer and connect their outputs to the next layer, which means that the neuron output connections of a layer with neurons belonging to the previous layer are not allowed. The layer of highest rank is called the output layer, and the intermediate layers between the input layer and the output layer are called hidden layers.

a. Monolayer network

The structure of a monolayer network (single layer network) is such that neurons organized as input are fully connected to other neurons organized at the output by modifiable weights.

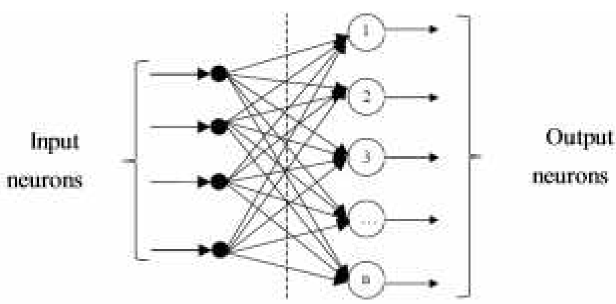

Figure III.2- Monolayer Network

b. Limitation of monolayer networks

Single-layer networks have paved the way for many applications, for example, they can represent the functions: AND and OR, but they have been unable to represent the XOR function, these limitations have been highlighted by Minsky and Papert in 1969.

The following figure shows the inability of the single-layer network to reproduce the XOR function.

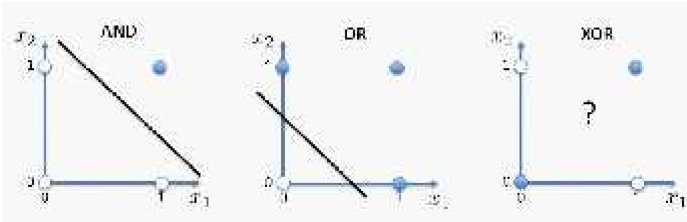

Figure III.3- Geometric representation of the XOR problem

This problem can be solved with the appearance of multilayer networks.

c. Multilayer network

The neurons are arranged by layer figure III.4. There is no connection between neurons of the same layer, and connections are only made with the neurons of the downstream layers.

Usually, each neuron in a layer is connected to all neurons in the next layer. This allows us to introduce the notion of the information direction (activation) within a network and thus define the concepts of input neuron, output neuron.

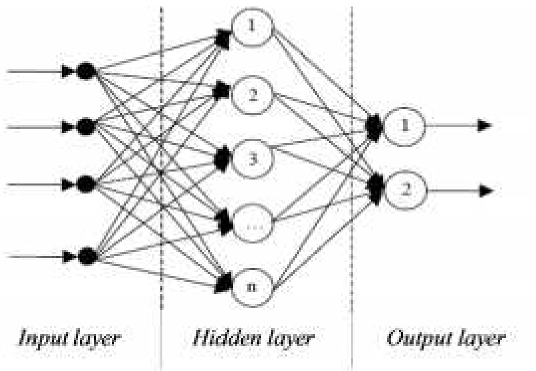

Figure III.4 - Multilayer network

III.2.4 Neural networks models

III.2.4.1 The perceptron model

The perceptron mechanism was invented by psychologist Frank Rosenblatt in the late 1950s [ROS 57]. It is monolayer with a threshold activation function.

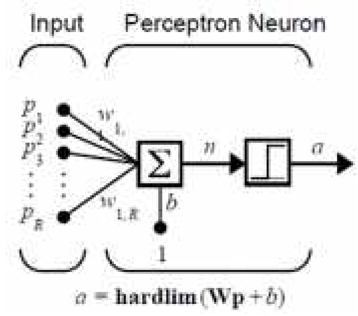

Figure III.5 - Perceptron model network

The perceptron neuron produces a 1 if the net input into the transfer function is equal to or greater than 0; otherwise it produces a 0. The hard-limit transfer function gives a perceptron the ability to classify input vectors by dividing the input space into two regions. Specifically, outputs will be 0 if the net input *n* is less than 0, or 1 if the net input *n* is 0 or greater.

III.2.4.2 The multilayer perceptron (MLP)

The multilayer perceptron (MLP) is a network comprising one or more hidden layers between the input layer and the output layer. In this type of networks, information flows only in one direction. In fact, each neuron of a layer is fully connected to the neurons of the next layer. Figure (III.6) gives an example of a MLP composed of an input layer, two hidden layers and an output layer.

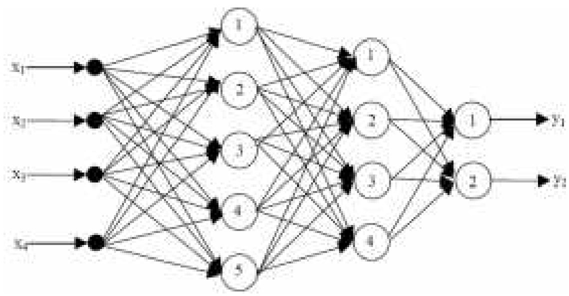

Figure III.6 - Example of multilayer perceptron

Multilayer networks are more powerful than single layer networks. For example, a network with two layers with a first sigmoid layer and a second linear layer may be raised to properly approximate many functions [BEN 09]. While a single layer network can not.

Practically, most networks have only 2 or 3 layers. Once created, the neural network is used according to the following protocol:

1. Initialization of weights and biases.
2. Learning with a known database.
3. Simulation or testing with new data.

III.2.5 Learning neural networks

Learning is probably the most interesting property of neural networks. It is a phase in the development of a neural network in which the network behavior is changed until the desired behavior is obtained. During this phase, the network adapts its structure (most often the connection weights) in order to provide on its output neurons the desired values. This learning requires examples also referred to as learning samples.

In terms of learning algorithms, two main classes have been defined according to whether the learning is said to be supervised or unsupervised. This distinction is based on the form of the learning examples.

III.2.5.1 Supervised Learning

The learning is supervised when the examples consist of pair values, type (input, desired output) [WEI 03]. The network must adapt by calculating its weights so that its output corresponds to the desired output (Figure III.7).

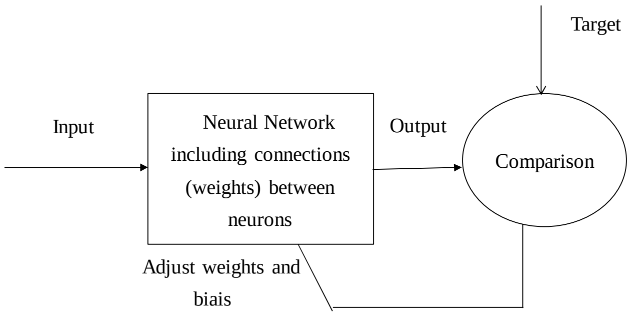

Figure III.7 - General diagram of supervised learning in neural networks

III.2.5.2 Unsupervised Learning

Learning is qualified as unsupervised when only input values are available. In this case, the examples presented at the input cause a self-adaptation of the network (Figure III.8) in order to produce output values that are close in response to similar input values (of the same nature) [CAU 05].

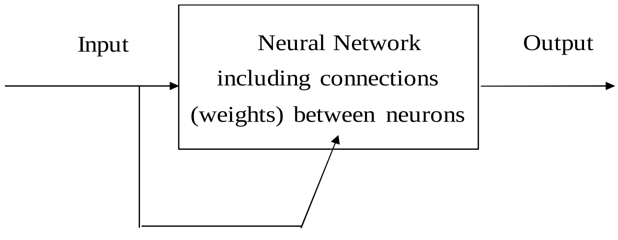

Figure III.8 - General diagram of unsupervised learning in neural networks

III.2.6 Learning by back-propagation algorithm

In the case of multilayer neural networks with a non-linear transfer function, the learning must be carried out by an algorithm of the error back-propagation. The algorithm is often referred to as retropropagation is the most popular among the learning techniques for multilayer networks. This algorithm is based on the generalization of the Pineda rule [PIN 87] using a sigmoid activation function. The network used is a layered network where each neuron is connected to the set of neurons in the next layer. The principle of this algorithm is the propagation of a signal from the input nodes to the output, then the error committed is propagated from the output to the internal layers up to the input [RUM 86] in order to calculate the new weight matrix.

The error back-propagation algorithm consists of the following steps:

1. Initialization of connection weights to random variables of small quantities.
2. Presentation of an example pair (input / output) of the learning database.
3. Calculation of the output by the example propagation.
4. Calculation of the different error signals for the different layers.
5. Updating the connection matrices.
6. As long as the error is very important, return to step 2.

$$E = \frac{1}{N}\sum_{k=1}^{N} e(k)^2 = \frac{1}{N}\sum_{k=1}^{N} (t(k) - a(k))^2 \qquad \text{(III.2)}$$

Where E: represents the squared error at the output of the network.

N: The number of examples in the learning database.

$e(k)$: The squared error committed at the output of the network.

$t(k)$: The target vector (desired output).

$a(k)$: The output vector developed by the network.

The optimal network weighting mechanism is based on the minimization of the error E, which leads to the j^{th} weight update equation of the following i^{th}neuron:

$$w_{ij}(k+1) = w_{ij}(k) + \alpha \frac{\partial E}{\partial w_{ij}(k)} \qquad \text{(III.3)}$$

Where α: Learning rate.

$w_{i,j}(k + 1)$: New weight.

$w_{i,j}(k)$: Old weight.

III.2.7 Learning Speed of neural networks

The learning speed is related to the forming process of a neural network. It is a function of the coefficient used to define the proportion in which the connection weights are modified at each iteration of the learning algorithm. If this learning coefficient chosen is very low, the algorithm has strong chances to converge, but it may need a large number of iterations and thus a lot of time for this (Figure III.9.a) [LON 12]. Conversely, if this learning coefficient is large, the algorithm is likely to converge rapidly but it may also diverge (Figure III.9.b).

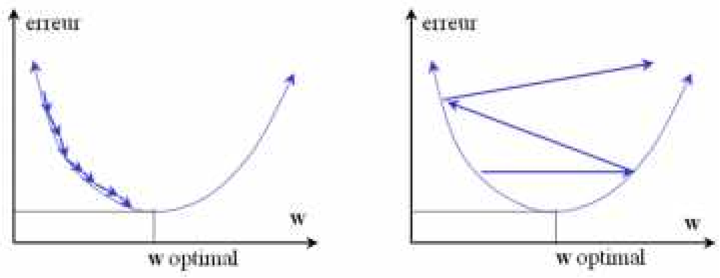

a) *b)*

Figure III.9 - Illustration of the learning speed effect of a neural network: a) slow convergence of the algorithm when the speed is low, b) divergence of the algorithm due to a learning speed too large

III.2.8 Neural network advantages and disadvantages

a. Advantages

The main qualities of neural networks are their capacity for adaptability and self-organization and the possibility of solving non-linear problems with a good approximation [WAT 87, ANA 92]. They have good noise immunity. The speed of execution is an important quality. These qualities have made it possible to achieve successfully several applications: classification, filtering, data compression, controller, etc...

b. Disadvantages

The difficulty of interpreting the neural network behavior is a disadvantage for the development of an application, these networks is a black box that does not explain its decisions. The neural network implementation is also a problem, where there are no rules that determine the structure of the network (number of layers, number of neurons in each layer, the initial parameters ...).

III.3 Deep learning method

Deep learning is a key component in today's state of the art applications using machine learning to conduct pattern recognition in images, video, and sound. It is proving superior to past pattern recognition approaches due to its improved ability to classify, recognize, detect, and describe data. The primary algorithm used to perform deep learning is the artificial neural network (ANN) [HAL 16]. Large volumes of data are often needed to train these networks, so when the number of layers increases a lot of computational power is needed to solve deep learning problems. Because of recent advances in research and computational power, we can now build neural nets with many more layers than just a few years ago.

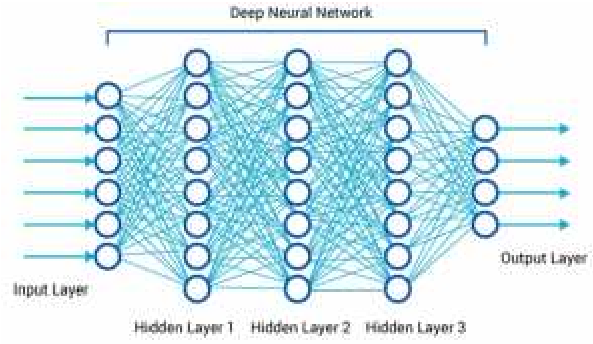

Figure III.10 - Deep learning architecture

By definition, deep learning is a set of algorithms in machine learning that attempt to learn in multiple levels, corresponding to different levels of abstraction. It typically uses artificial neural networks. The levels in these learned models correspond to distinct levels of concepts, where higher-level concepts are defined from lower-level ones, and the same lower level concepts can help to define many higher-level concepts [DEN 13].

III.3.1 Deep networks training

Deep architectures, such as artificial neural networks with many hidden layers, usually need to be trained in two stages. The first part of the training process is so called pretraining, which aims typically at building deep feature hierarchy, and is performed in an unsupervised mode. The latter stage is supervised fine tuning of the network parameters.

Optimizing a training criterion for deep architectures is a very difficult task. As it was experimentally demonstrated [VIN 10], for hundreds random initializations, the gradient-based training process may lead to hundreds different local minima. This is why an additional mechanism to regular optimization is required. The network is initialized with the use of unsupervised algorithm, which helps in obtaining better generalization after the network is learned.

III.3.1.1 Deep network pretraining

Typically, in a supervised learning task, a deep neural network is initialized with random weights. Performing back-propagation directly on a freshly initialized network will tend to be very slow and get stuck in poor local minima as the loss function is parameterized by millions of free variables with complex dependencies. This leads to deep neural networks that take a long time to train and yield poor results. In his highly influential work on deep networks, Hilton [HIL 06] showed that if you pretrain each layer of the network in an unsupervised manner to learn a sparsified representation before the classification task the learning problem was greatly reduced.

Two main algorithms are applied. The most popular Deep Belief Networks consisting of Restricted Boltzmann Machines (RBM) are trained layer by layer with so called Contrastive Divergence and its variants [CAR 05, TIE 09], while stacked autoencoders [VIN 10] are made of feedforward layers previously trained to reconstruct their inputs. We focus in our study only on stacked autoencoders pretraining.

III.3.1.2 Autoencoder

An autoencoder or an autoassociator is an artificial neural network used for unsupervised learning of efficient coding. The aim of an autoencoder is to learn a representation (encoding) for a set of data, typically for the purpose of dimensionality reduction.

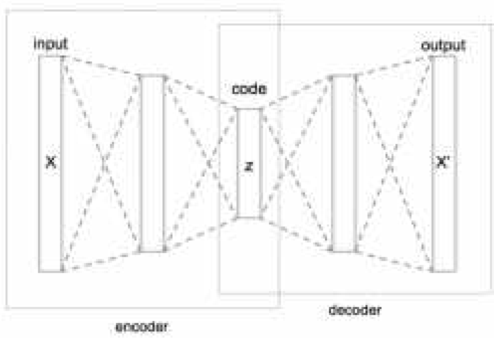

Figure III.11 - Schematic structure of an autoencoder with

3 fully-connected hidden layers

Architecturally, the simplest form of an autoencoder is a feedforward, non-recurrent neural network very similar to the multilayer perceptron (MLP) having an input layer, an output layer and one or more hidden layers connecting them, the output layer having the same number of nodes as the input layer, and with the purpose of reconstructing its own inputs, instead of predicting the target value.

An autoencoder always consists of two parts, the encoder and the decoder, which can be defined as transitions ϕ and ψ such that:

$$\phi: \mathcal{X} \longrightarrow \mathcal{F}$$

$$\psi: \mathcal{F} \longrightarrow \mathcal{X}$$

In the simplest case, where there is one hidden layer, the encoder stage of an autoencoder takes the input $x \in \mathbb{R}^d = \mathcal{X}$ and maps it to $z \in \mathbb{R}^p = \mathcal{F}$

Where:

$$Z = f \;\; wx + b \qquad \text{(III.4)}$$

This image Z is usually referred to as code, latent representation. Here, f is an activation function such as a sigmoid function. w is a weight matrix and b is a bias vector. After that, the decoder stage of the autoencoder maps Z to the reconstruction x' of the same shape as x :

$$x' = f' \;\; w'Z + b' \qquad \text{(III.5)}$$

Where f', w', b' for the decoder may differ in general from the corresponding f, w, b for the encoder, depending on the design of the autoencoder.

Autoencoders are also trained to minimise reconstruction errors such as squared errors:

$$E = \|x - x'\|^2 = \|x - f'(w'f(wx + b) + b')\|^2 \qquad \text{(III.6)}$$

III.3.1.2.1 Autoencoder training

The training algorithm for an autoencoder can be summarized as

1. For each input x, a feed-forward pass to compute activations at all hidden layers, then at the output layer to obtain an output x'.
2. Measure the deviation of $x'$from the input x (typically using squared error).
3. Backpropagate the error through the net and perform weight updates.

Stacking autoencoders so that each layer of the network learns an encoding of the layer below creates a network that can learn hierarchical features in an unsupervised manner [VIN 10]. It turns out that training stacked layers in this manner allows a deep network to learn a good representation incrementally instead of trying to train the whole network in ensemble from a random initialization of weights.

III.4 Hybrid learning method

The modern techniques of artificial intelligence have found application in almost all the fields of the human knowledge. However, a great emphasis is given to the accurate sciences areas, perhaps the biggest expression of the success of these techniques is in engineering field [ALT 92, ASA 94]. Neural networks and fuzzy logic, these two techniques are many times applied together for solving engineering problems where the classic techniques do not supply an easy and accurate solution. The neuro-fuzzy term was born by the fusing of these two techniques.

III.4.1 Neuro-fuzzy networks

Still there is no absolute consensus but in general, the neuro-fuzzy term means a type of system characterized for a similar structure of a fuzzy controller where the fuzzy sets and rules are adjusted using neural networks tuning techniques in an iterative way with data vectors (input and output system data).

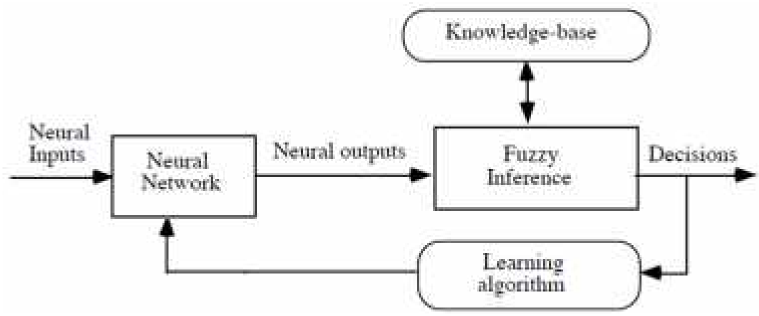

Figure III.12 - The fuzzy neural system

Such systems show two distinct ways of behavior. In a first phase, called learning phase, it behaves like neural networks that learns its internal parameters off-line. Later, in the execution phase, it behaves like a fuzzy logic system. Separately, each one of these techniques possess advantages and disadvantages that, when mixed together, their cooperage provides better results than the ones achieved with the use of each isolated technique.

III.4.2 Fuzzy Systems

Fuzzy systems propose a mathematic calculus to translate the subjective human knowledge of the real processes. This is a way to manipulate practical knowledge with some level of uncertainty. The fuzzy sets theory was initiated by LOTFI ZADEH [ZAD 65], in 1965. The behavior of such systems is described through a set of fuzzy rules, like:

IF "premise" THEN "consequent", that uses linguistics variables with symbolic terms. Each term represents a fuzzy set.

III.4.3 Fuzzy logic theory

Fuzzy sets, fuzzy operators and the knowledge base are building blocks of fuzzy logic theory.

III.4.3.1 Membership function

Fuzzy sets are represented by membership functions [VAL 07]. A particular element of the fuzzy set will have grade of membership which gives the degree to which a particular element belongs to a set. A membership function is a curve that provides the degree of membership within a set of any element that belongs to the universe of discourse X. If X is the universe of discourse and the elements in X are denoted by x, then a fuzzy set A in X is defined as a set of ordered pairs.

$$A = \{x, \mu_A(x); x \in X, \mu_A(x) \in [0,1]\} \tag{III.7}$$

Where $\mu_A(x)$ is a membership degree of x in A shown in figure III.13

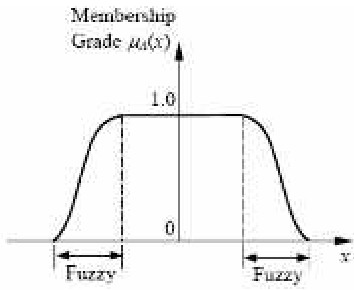

Figure III.13 - The membership function of a fuzzy set

III.4.3.1.1 The membership function types

There are different types or forms of membership functions of a fuzzy set. The most commonly used types are shown below [AYO 12].

a. Triangular membership function

A triangular membership function, as illustrated in figure III.14, is characterized by three parameters x_1, x_3 and x_2 corresponding respectively to the lower bound, the upper bound and a modal value. This type of function is defined as follows:

$$\mu_A(x) = \begin{cases} \dfrac{x - x_1}{x_2 - x_1} & if\ x_1 \leq x < x_2 \\ \dfrac{x - x_3}{x_2 - x_3} & if\ x_2 \leq x < x_3 \\ 0 & otherwise \end{cases} \tag{III.8}$$

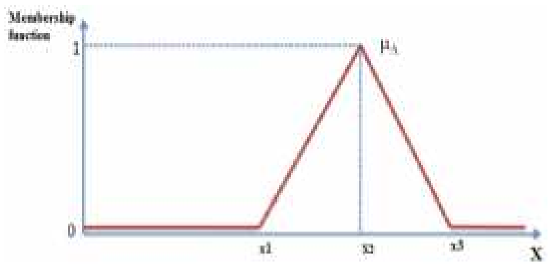

Figure III.14 - Triangular membership function

b. Trapezoidal membership function

A trapezoidal membership function, as illustrated in figure III.15, is defined by four parameters x_1,x_2, x_3 and x_4. The parameters x_1 and x_4 represent respectively the lower limit and the upper limit of the support. The parameters x_2 and x_3 are respectively the lower bound and the upper bound of the core. This function is defined by the following expression:

$$\mu_A(x) = \begin{cases} \frac{x - x_1}{x_2 - x_1} & if\ x_1 \leq x < x_2 \\ 1 & if\ x_2 \leq x < x_3 \\ \frac{x - x_4}{x_3 - x_4} & if\ x_3 \leq x < x_4 \\ 0 & otherwise \end{cases} \quad \text{(III.9)}$$

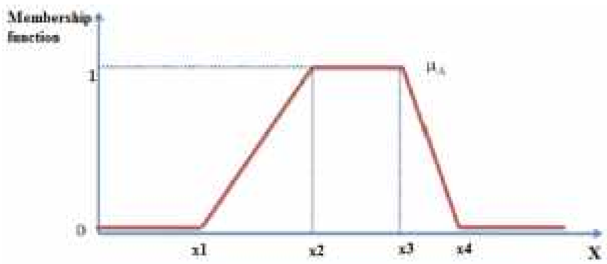

Figure III.15 - Trapezoidal membership function

c. Gaussian membership function

A Gaussian membership function, as illustrated in figure III.16, is characterized by its central value m and its standard deviation σ. The Gaussian membership function is defined by:

$$\mu_A(x) = exp\left[-\frac{1}{2}\left(\frac{x - m}{\sigma}\right)^2\right] \quad \text{(III.10)}$$

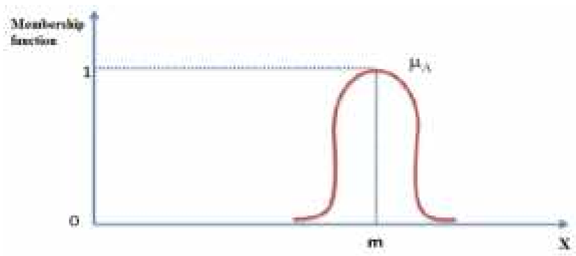

Figure III.16 - Gaussian membership function

III.4.3.2 Fuzzy operators

Boolean operators such as "AND", "OR" and "NOT" operators exist in fuzzy logic as well. These operators are defined as the minimum, maximum and complement.

III.4.3.3 The knowledge base

The knowledge base in fuzzy logic is represented by if-then rules of fuzzy descriptors. A single "IF-THEN" rule assumes the following format:

$$if\ x\ is\ A\ then\ y\ is\ B$$

A and B are linguistic variables and are defined by fuzzy sets on the ranges X and Y (where X and Y are the universes of discourse).

The "if " part of the rule "x is A" is the antecedent or premise and the "then" part of the rule "y is B" is the consequence or conclusion.

III.4.4 Fuzzy inference mechanism

The fuzzy inference mechanism consists of three stages:

1. In the first stage, the values of the numerical inputs are mapped by a function according to a degree of compatibility of the respective fuzzy sets, this operation can be called Fuzzification.
2. In the second stage, the fuzzy system processes the rules in accordance with the firing strengths of the inputs.
3. In the third stage, the resultant fuzzy values are transformed again into numerical values; this operation can be called defuzzyfication.

Essentially, this procedure makes possible the use fuzzy categories in representation of words and abstracts ideas of the human beings in the description of the decision taking procedure.

III.4.5 The fuzzy systems advantages and disadvantages

The advantages of fuzzy systems are:

- Capacity to represent inherent uncertainties of the human knowledge with linguistic variables.
- Easy interpretation of the results, because of the natural rules representation.
- Easy extension of the base of knowledge through the addition of new rules.

And its disadvantages are:

- Incapable to generalize, or either, it only answers to what is written in its rule base.
- Not robust in relation the topological changes of the system, such changes would demand alterations in the rule base.
- Depends on the existence of an expert to determine the inference logical rules.

III.4.6 The ANFIS Model

ANFIS (Adaptive Network Based Fuzzy Inference System) is a neuro-fuzzy adaptive inference system that consists of using a MLP neuron network with 5 layers, each layer corresponds to the realization of a stage of a fuzzy inference system, TAKAGI SUGENO type. For simplicity, we assume that the fuzzy inference system with two inputs x and y, and as an output Z. Suppose the rule base contains two fuzzy rules Takagi-Sugeno type.

Rule1: $if\ x\ is\ A_1\ and\ y\ is\ B_1\ then\ Z_1 = p_1x + q_1y + r_1$ (III.11)

Rule2: $if\ x\ is\ A_2\ and\ y\ is\ B_2\ then\ Z_2 = p_2x + q_2y + r_2$ (III.12)

Where A_i and B_i are fuzzy sets, p_i, q_i and r_i are the consequent parameters that are determined. The ANFIS architecture is equivalent to five layers as shown in figure III.17.

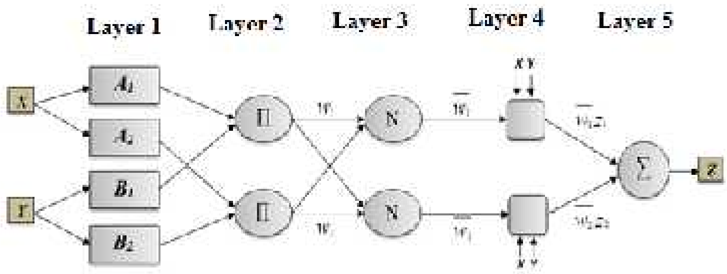

Figure III.17 - General architecture of ANFIS

A typical architecture can be described as follows:

1. The first layer of ANFIS architecture comprises as many neurons as there are fuzzy subsets in the inference system represented. Each neuron calculates the degree of truth of a particular fuzzy subset by its transfer function.

   The activation functions of the neurons i of the first layer:

$$Z_i^1 = \mu_{Ai}\ x \tag{III.13}$$

As x is the input to the neuron i, and A_i is a fuzzy subset corresponding to the variable x. In other words, Z_i^1 is the membership function of A_i and it indicates the degree to which x satisfies the quantifier A_i.

2. In the second layer, every neuron is fixed, and the circle node is labeled as π. The output neuron is the result of multiplying of signals coming into this neuron and delivered to the next neuron. Each neuron in this layer represents the firing strength for each rule. In this layer, the AND operator, is applied to obtain the output

$$w_i = \mu_{Ai} \square \mu_{Bi} \tag{III.14}$$

Where w_i is the output that represents the firing strength of each rule.

3. The third layer normalizes the activation degree of the rules. Every neuron in this layer is fixed and the circle node is labeled as N. Each neuron is a calculation of the ratio between the i^{th} rules firing strength and the sum of all rules firing strengths. This result is known as the normalized firing strength.

$$\overline{w}_i = \frac{w_i}{\sum_i w_i} \tag{III.15}$$

4. The fourth layer is used to determine the consequence parameters to the rules. Every node in this layer is an adaptive neuron to an output, with a node function defined as:

$$\overline{w}_i Z_i^4 = \overline{w}_i\ \ p_i x + q_i + r_i \tag{III.16}$$

Where $\overline{w}_i$ is the normalized firing strength from the previous layer (third layer) and p_i, q_i, r_i is a parameter in the node. The parameters in this layer are referred to as consequent parameters.

5. The fifth layer is the output layer which contains a single fixed neuron that computes the overall output as the summation of all incoming signals from the previous neurons. In this, a circle node is labeled as Σ

$$Z^5 = \ _i\ \overline{w}_i\ Z_i^4 \tag{III.17}$$

III.4.7 Hybrid learning algorithm

In the ANFIS architecture, the first layer and the fourth layer contain the parameters that can be modified over time. In the first layer, it contains a nonlinear of the premises parameter while the fourth layer contains linear consequent parameters. To update both of these parameters required a learning method that can train both of these parameters and to adapt to its environment. A hybrid algorithm proposed by Jang (1993) [JAN 93] will be used in this study to train of these parameters.

There are two parts of a hybrid learning algorithm, namely the forward path and backward path. In the course of the forward path, the parameters of the premises in the first layer must be in a steady state. A recursive least square estimator (RLSE) method was applied to repair the consequent parameter in the fourth layer. Next, after the consequent parameters are obtained, input data is passed back to the adaptive network input, and the output generated will be compared with the actual output.

While backward path is run, the consequent parameters must be in a steady state. The error occurred during the comparison between the output generated with the actual output is propagated back to the first layer. At the same time, parameter premises in the first layer are updated using learning methods of gradient descent.

III.4.8 ANFIS advantages

1. Exploitation of the knowledge available, thanks to the rule base.
2. Reduction of the rule base size: it is enough to have general rules; the details will be provided by the RN.
3. Immediate effectiveness from the beginning of learning and the possibility to avoid erratic initial behavior.
4. Fast convergence time.

III.5 Conclusion

This chapter explains in detail the theoretical background of the machine learning methods, which are: artificial neural networks, deep learning and hybrid learning methods.

We gave an overview of different topologies for ANN. Their implementation depends primarily on the nature of the problem to be treated (function approximation, classification, pattern recognition...). Once the problem is properly addressed, it is necessary to choose an appropriate network structure and learning algorithm.

Nevertheless, we note that for our study (crack characterization) we will limit ourselves to the use of the gradient retropropagation algorithm applied to the MLP.

Deep learning method which describes a category of algorithms that use a pipeline of neural networks to learn a hierarchy of features, typically for classification tasks. Stacking autoencoders so that each layer of the network learns an encoding of the layer below creates a network that can learn hierarchical features in an unsupervised manner. It turns out that training stacked layers in this manner allows a deep network to learn a good representation.

The techniques based in fuzzy logic and neural networks are frequently applied together. The reasons to combine these two paradigms come out of the difficulties and inherent limitations of each isolated paradigm. This type of system is characterized by a fuzzy system where fuzzy sets and fuzzy rules are adjusted using input output patterns. There are several different implementations of neuro-fuzzy systems, where each author defined its own model. In this approach, we focused on the area describing the ANFIS model, its structure, learning algorithm and advantages.

In the following chapter, we present the experimental validation of these three different approaches for nondestructive testing by eddy current of cracks embedded in conductive structures.

CHAPTER IV

CRACK CHARACTERIZATION USING MACHINE LEARNING METHODS

IV.1 Introduction

In the construction industry, non destructive testing (NDT) methods are gaining more popularity for their ability to examine the materials, components, systems properties. NDTs are typically much cheaper and faster comparing to traditional destructive tests. In addition, the NDT will not cause any damage to the structure components. There are many NDT technologies that are available for inspections; eddy currents testing (ECT) [PEI 02] is one of the NDT methods that are widely used in detecting surface or subsurface crack of conductive materials. Recent technologies have made ECT more powerful and useful in quality assurance.

Knowledge of defect size is a very important parameter for the engineer, in order to allow him to decide the future of the part, most NDT methods do not reveal much about the shape of the defect. Currently there is a strong demand for a more quantitative than qualitative characterization of the defects that is to say to carry out a nondestructive testing in order to reconstruct the defect parameters. In this case we speak of the inverse problem, usually difficult to solve.

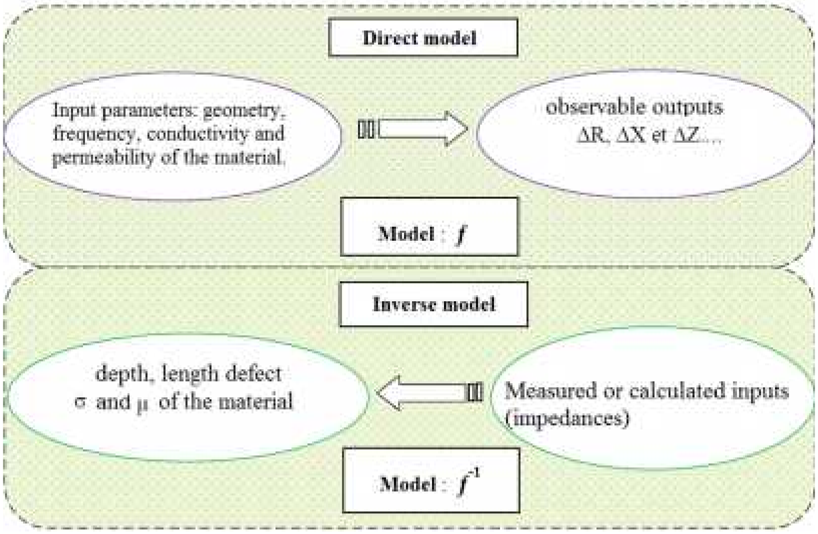

Figure IV.1 - Direct and inverse problems

Faced with this need to find solutions to inverse problems, several methods have emerged in order to remedy these problems. These methods are part of machine learning which is one of the fastest growing areas of computing. It is not only that the data are constantly "bigger", but also the theory of treating them and transforming them into knowledge.

In this part, we will cite some machine learning methods for solving the inverse problem, among them we mention: artificial neural networks PML, deep learning, and hybrid machine learning method. These different methods used for the crack evaluation are implemented as the software MATLAB

IV.2 Calculation of the eddy current probe impedance

The forward problem consists in the determination of the crack in the plate by the variation of the probe impedance. The impedance change of the coil reflects the change in permeability distribution in a test specimen in the presence of defects. The coil is excited by an alternative current of angular frequency ω, its impedance is measured as a function of frequency in scanning positions. The eddy current problem can be described mathematically by the following partial differential equation in terms of the magnetic vector potential [PAL 83] [IDA 88].

$$rot \ \frac{1}{\mu} rot \ \vec{A} = -\frac{\partial \vec{A}}{\partial t} + gradv + j_s \qquad \text{(IV.1)}$$

Where $\vec{A}$: The magnetic vector potential.

V : the electrical scalar potential

ω: The angular frequency of the excitation current (rad/s).

μ: The magnetic permeability of the media involved (H/m).

σ: The electrical conductivity (S/m).

j_s: The current density (A/m^2).

j: The imaginary unit.

Once the magnetic vector potential values at all the nodes in the mesh region are determined, the probe impedance which is our parameter of interest can be computed. The real and imaginary parts of the probe impedance are determined by using the magnetic energy and the power losses, respectively [IDA 88].

$$P = RI^2 \quad et \quad W = \frac{1}{2} LI^2 \qquad \text{(IV.2)}$$

Hence, we can obtain the reactance and the resistance of the probe. And the source impedance can be written as:

$$Z = R + j\omega L = \frac{1}{I^2} \; P + j2\omega W \qquad \text{(IV.3)}$$

IV.3 Artificial neural networks

In recent years the artificial neural network (ANN) was to use in the non destructive testing where it's interviewee to inverse problem. But, the NDT requires the use of the numerical methods, among these methods, the finite element method (FEM). It appears to be very powerful because of its large flexibility which allows taking into consideration complex configurations. Their application is widely used to detect cracks in conductive structures by using the eddy currents [UDP 04].

The application of the ANN to electromagnetic inversion is used in the case of impedance measurement of the probe by eddy currents; the inversion method is investigated to estimate the map of defect [YAN 98]. The eddy current probe impedance variation is given as input to the artificial neural network and the geometric parameters of crack are evaluated continuously by output of the ANN.

IV.3.1 Implementation of the artificial neural network

The application of ANN to the inversion method of the probe impedance is trained and tested to identify and evaluated the geometric parameters of the crack, which are particularly in our case the length and depth. The ANN input consists in the probe impedance variation while its output provides evaluated cracks with different lengths and depths.

An important problem in the ANN inversion process is the selection of the network structure and the adjustment of its internal parameters. In order to develop an optimal neural network structure, we have carried out several experiments by varying the settings of the network, such as the activation function, the number of hidden layers, the number of neurons in each layer, the learning algorithm. Finally, our choices are oriented in this way:

a. The choice of the neural network type

Feed-forward back propagation neural networks are a class of networks that are widely used for solving function approximation problems and it's used for the resolution of the nonlinear problems. This structure is composed of separate layers including an input layer, a hidden layer and an output layer. The training is based on simulated data, involving the impedance of the probe coil, which is determined by the finite elements method.

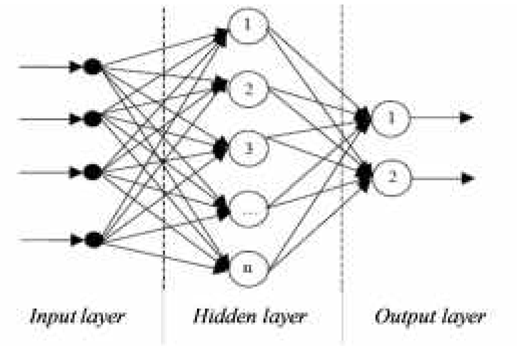

Figure IV.2- Feed-forward neural network

The training consists in the adjustment of the layer weights values for the output neural network. This weight adjustment process is repeated for many training samples, and is stopped when the errors at the output layer reach a sufficiently low level [HAG 94].

b. The choice of the learning strategy

Learning is a very important property of neural networks, in our case we have chosen supervised learning, let us recall that the learning is said to be supervised when the examples are constituted by a couple of values, type (input / output). The network then has to adapt, by calculating its weights so that its output corresponds well to the desired output, so we have chosen the "batch training" mode, which means that the synaptic weights will be modified only after the presentation of all the learning base examples. Currently, several learning algorithms are developed, our choice is oriented towards, the Levenberg-Marquardt algorithm, which leads to faster convergence than other first-order algorithms [YAS 02].

c. The choice of the cost function

The selected cost function is the mean square error MSE, reflecting the gap between the network output and the desired output, it’s defined by:

$$MSE = \frac{1}{N}\sum_{k=1}^{N} e(k)^2 = \frac{1}{N}\sum_{k=1}^{N} (t(k) - a(k))^2 \qquad \text{(IV.4)}$$

Where N: The number of examples in the learning database.

$e(k)$: The squared error committed at the output of the network.

$t(k)$: The target vector (desired output).

$a(k)$: The output vector elaborated by the network.

The adjust of the neural network internal parameters is performed by minimizing the mean square error (MSE).

IV.3.2 Development of the learning database

The choice of the learning base is a very important step that must not be neglected, and which directly influence the results obtained. The training base used in our work was developed from the simulation results by the finite element method and experimental results of reference [HEL 12], we use the signature of the crack, which contains a range of measures. For this purpose, instead of using a single measurement corresponding to a single position, we use a set of measurements corresponding to a multitude of positions. It is evident that this signature represents completely the crack.

A vector composed of 42 numerical measurements representing the resistance variation and the reactance variation corresponding to 21 different positions along the crack constitutes the ANN input vector.

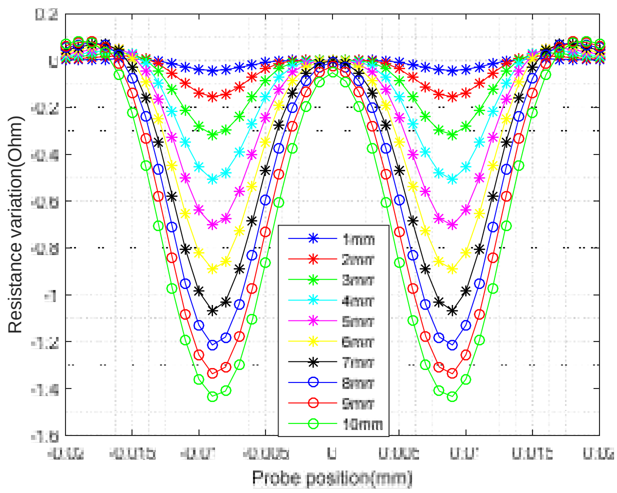

Figure IV.3- Resistance variation as a function of the probe position for different crack lengths of the same thickness (0.20 mm) and the same depth (2 mm)

Figure IV.3 shows clearly that it is not appropriate to take an input vector consisting only a one value of the impedance variation. By this approach we undoubtedly overcome the uniqueness of the solution problem.

For the inversion problem, two databases were used. Each database contains examples of the ANN input-output. These bases are the learning base and validation base. For this application, these bases are constituted respectively by 50 and 10 examples, such that the inputs are the impedance variations and the desired outputs are the crack lengths and the crack depths.

IV.3.3 Crack detection for different length using the finite element results

The variation of the impedance as a function of the probe position for different crack lengths is given by the following two figures show the resistance variation and the reactance variation produced by cracks of the same thicknesses (0.20 mm) and the same depth (2mm).

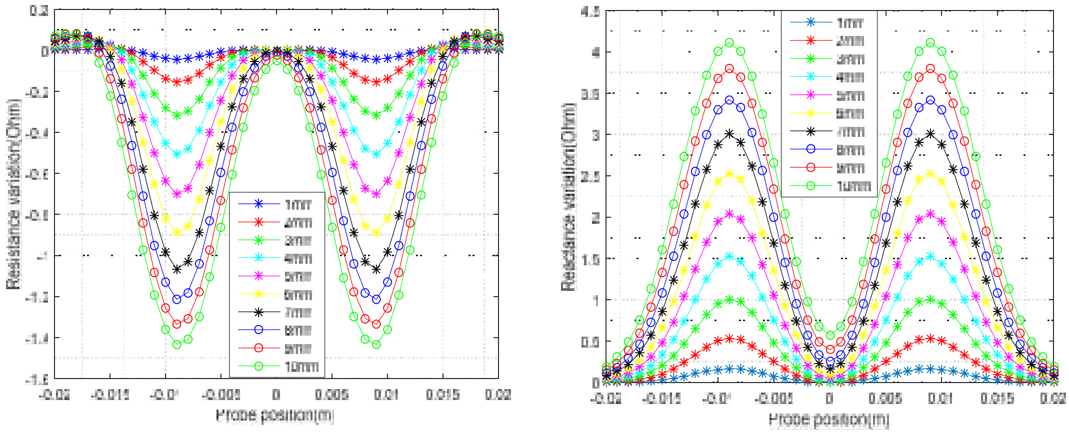

a) ***b)***

Figure IV.4- a) Resistance variation, b) reactance variation: as a function of the probe position for different crack lengths of the same thickness (0.20 mm) and the same depth (2mm)

IV.3.4 Evaluation of the crack lengths by artificial neural network PML

The artificial neural network for evaluating of the crack lengths is a perceptron multilayers PML consists of (10) neurons in the hidden layer with a hyperbolic tangent activation function and an output neuron with a linear activation function, the network receives at its input the impedance variation values and supplied at its output the crack lengths values. This network will be trained from the learning base created by the finite element calculation.

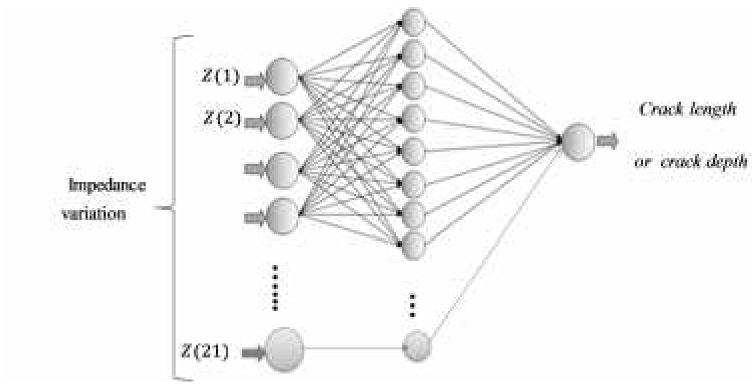

Figure IV.5 - Implementation of the neural network using for the estimation of geometric parameters

During the learning phase, the desired output is compared with the output developed by the network, and the error committed will be minimized thanks to the Levenberg-Marquardt minimization algorithm.

After a little pre-10 passes of the learning base, and a learning rate equal to 0.01, the algorithm converges towards the minimum tolerated error, while adjusting the weights and biases values of the network. Once the weights and the biases are adapted, we recover the values of the estimated crack length at the network output, the results obtained are presented as follows:

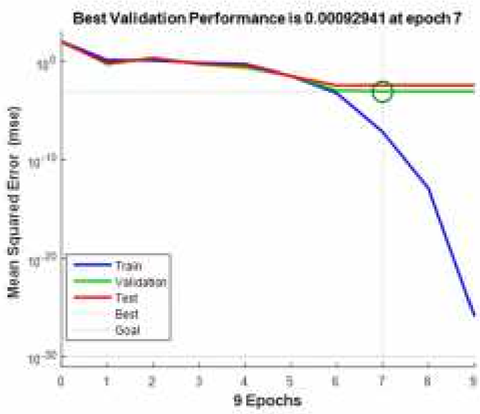

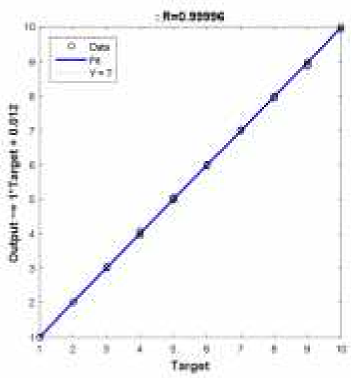

a) ***b)***

Figure IV.6 - a) MSE on learning and validation bases, b) correlation between the desired output and the network output for the crack lengths

The figures IV.6-a and IV.6-b respectively represent the evolution of the cost function which is in our case defined by the mean square error, we notice that it decreases according to the number of iterations until it arrives at the minimum that we have imposed 10^{-30}, that the second figure represents the linear regression between the real output and the output estimated by the neural network, we note a good correlation between the values.

IV.3.4.1 Validation of results

The last step is to test the model's ability to generalize. Generalization is the ability of a neural network to achieve good forecasts when powered by data that are not from the training set (but from the same source as the training set). In this phase, the network capacity will be tested to find the parameters of the target (crack lengths) corresponding to examples of the impedance belonging to the area of learning.

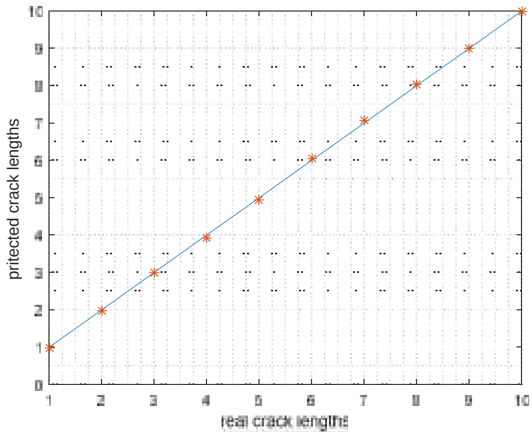

Figure IV.7 - Estimated lengths according to the real lengths of the crack

According to this figure, the ability of our neural network to generalize is well shown, so we conclude that the inversion by ANN is able to generalize and gives results with good accuracy, where the MSE is 0.0022.

IV.3.5 Crack detection for different depth using the finite elements results

In this case we developed a learning base from the experimental results of reference [HEL 12] to be used for the network training. The impedance variation of the probe as a function of the probe position for the different crack depths is given as follows:

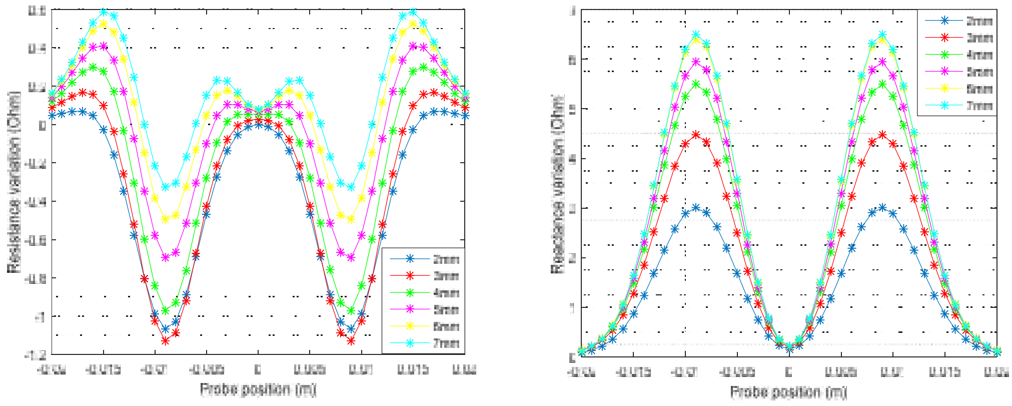

a) ***b)***

Figure IV.8 - a) Resistance variation, b) reactance variation: as a function of the probe position for different crack depths of the same thickness (0.20 mm) and the same length (7mm)

We notice in figure III.8 that the curves representing the resistance variation and reactance variation as a function of the probe position are no longer discernible beyond a certain depth which we will call depth limit. Thus, it is not possible to estimate the depths of the actual cracks exceeding these limiting depths.

IV.3.6 Evaluation of the crack depths by artificial neural network PML

For the evaluation of the various crack depths from 2mm to 7mm, we will adopt the same architecture of the neural network that used in the case of length reconstitution and also the same learning strategy, except that here the network output will be the different values of the depth, consequently the learning base will be changing and will be different for each depth.

After 74 passes of the learning base, a learning rate equal to 0.1 and a minimum error imposed at 10^{-12}, the network neuron weights and biases are adjusted.

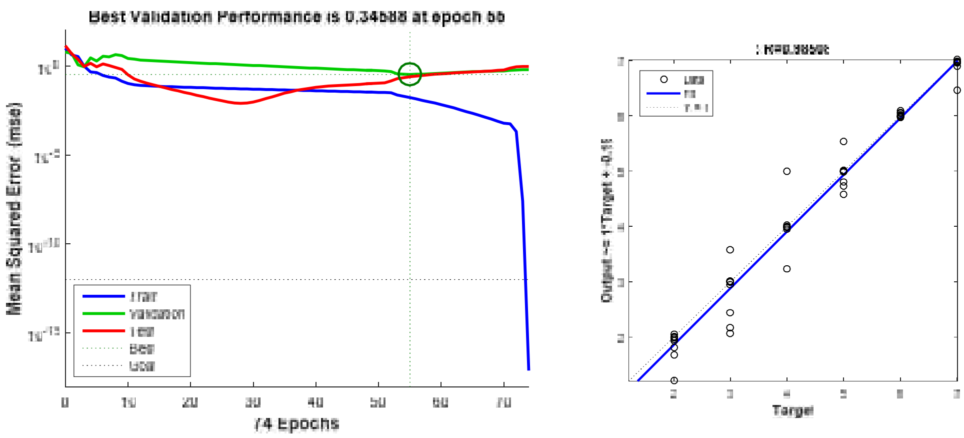

a) ***b)***

Figure IV.9 - a) MSE on learning and validation bases, b) correlation between the desired output and the network output for crack depths

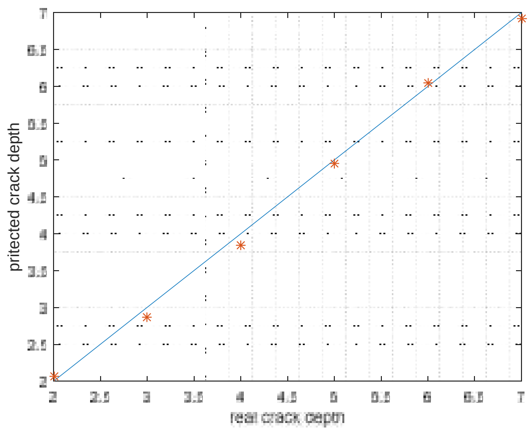

Figure IV.10 - Estimated depths according to the real depths of the crack

For the depth, we can say that our artificial neuron network has generalized, and the results show a good accuracy MSE = 0.0096.

IV.3.7 Optimization of the neural network topology

Our goal is to discover a network architecture that makes it possible to estimate both geometric parameters of the crack (length and depth) at a time, remember that there are no rules that can determine such a structure for such application, for this reason, we made several trainings, varying the different parameters of the network (number of neurons, activation function, the initial weights ...).

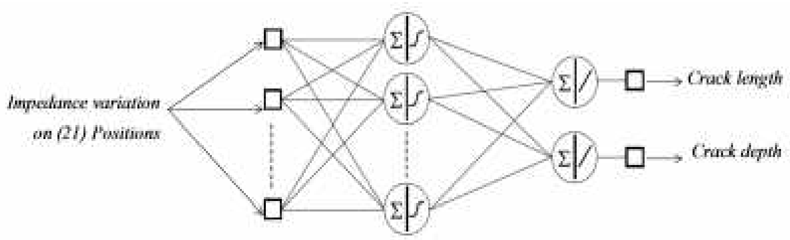

Figure IV.11 - Implementation of the neural network for length and depth crack outputs

The usual purpose of a model selection procedure is to determine the most efficient model in terms of performance, but also the most parsimonious in computation time. The artificial neuron network results of the lengths and depths outputs are shown in the following figures:

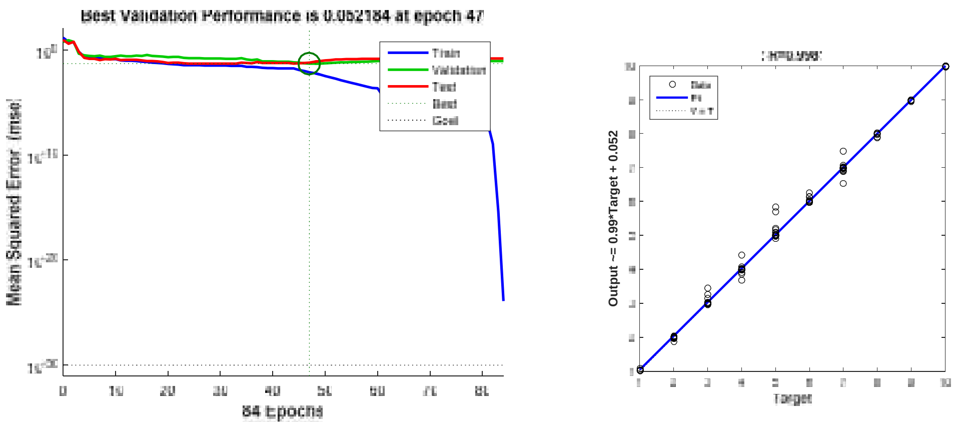

a) ***b)***

Figure IV.12 - a) MSE on learning and validation bases, b) correlation between the desired output and the network output for crack lengths and crack depths

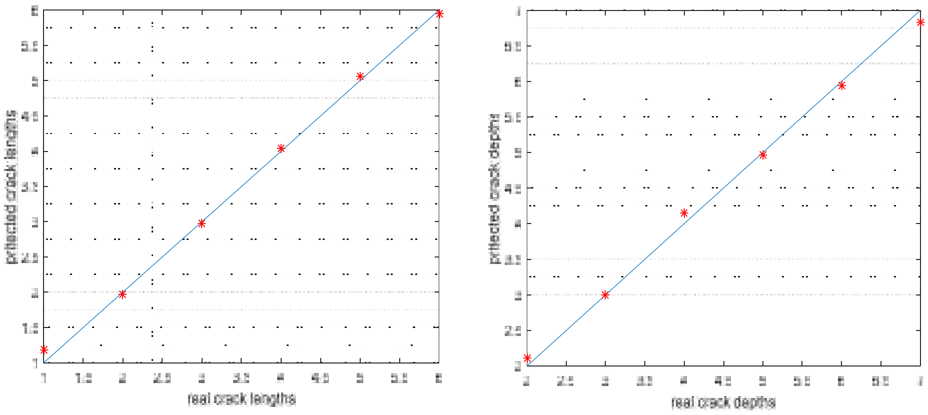

a) ***b)***

Figure IV.13 - Estimated neural network output according to the real output for the crack lengths and crack depths respectively

This network topology allows to achieve a performance translated by the MES which equals 0.0091. It is possible that there are several architectures more optimal than that used in our work, but the choice of the optimal parameters remains a critical choice.

IV.4 Deep learning method

The aim of this part is to present a novel machine learning method for estimating the crack parameters solving the invers problem. Recently, deep neural networks have demonstrated their ability to achieve excellent performance for classification tasks for big data, this networks type are a class of machine learning algorithm, which are no more than multilayer networks, of classical architecture, but they include several hidden layers and it is the way to manage their learning which gave, since 2006, a revival interest in their study. The problem of choosing hyper parameter is very critical for these networks because the size of the search space grows exponentially with the number of layers.

Deep learning use a cascade of many layers of nonlinear processing units for feature extraction and transformation, each successive layer uses the output from the previous layer as input. The algorithms may be supervised or unsupervised.

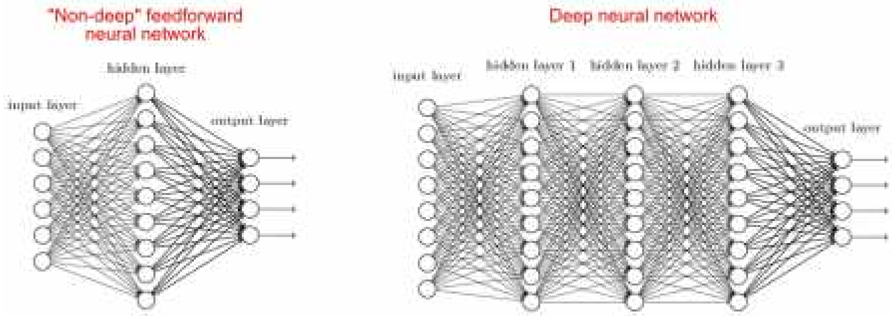

Figure IV.14 - Neural network and deep neural network

IV.4.1 Implementation of the deep neural network

Applying high dimensional row data directly to a machine learning algorithm often gives unsatisfactory results due to the curse of dimensionality therefore practitioners of machine learning algorithms first extract features from the data in order to capture relevant high level information and reduce the dimensionality of data and then apply the feature representations to the learning algorithm. The deep network uses unsupervised feature learning to construct its own features from unlabeled data.

IV.4.1.1 Module for deep learning

There are many different modules can be used for unsupervised feature learning and be stacked to construct deep network in our case we use the autoencoder, which composed of an encoder and a decoder, the goal of an autoencoder is to reconstruct the input data via one or more layers of hidden units. The encoder maps an input to a hidden representation and the decoder attempts to reverse this mapping to reconstruct the original input.

IV.4.1.2 Topology optimization by unsupervised criteria

Our objective is to discover an optimal number of neurons, layer by layer; this requires being able to compare different topologies with an unsupervised criterion. It is possible that there are several or even an infinity of global optimums. The usual purpose of a model selection procedure is to determine the most efficient model in terms of performance, but also the most parsimonious in computation time. We will therefore try to establish a lower bound on the number of neurons necessary for each hidden layer.

It is found that the best performance is obtained for the configurations having a minimum of 50 neurons in the first hidden layer. Moreover, once this minimum reached, adding more neurons does not significantly increase performance. This observation validates our choice of determining a lower bound for the optimal size of the first hidden layer at 50 neurons.

We optimize the size of the second layer after fixing the first hidden layer size according to the previous optimum (50 neurons). The optimal number of neurons for the second hidden layer is bounded lower by 60 neurons. In the same way as for the first layer, adding more neurons does not significantly improve performance.

IV.4.2 Evaluation of the crack lengths by deep network

Using the topology optimized previously, to restore the various lengths of defects, we train the hidden layers individually in an unsupervised fashion using autoencoders, and we join the layers together to form a deep network, which is trained one final time in a supervised fashion, the results show a good accuracy between values, and the confusion matrix proved that.

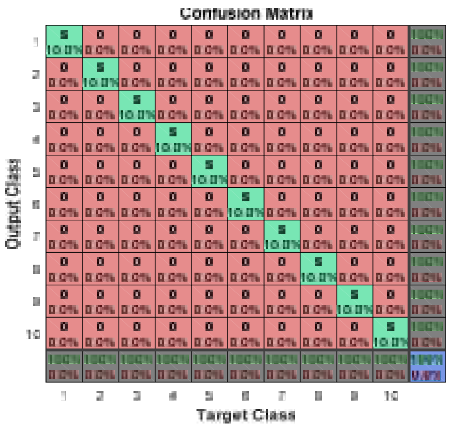

Figure IV.15 - Correlation between the desired output and the deep network output for crack lengths

The figure IV.15 which is the confusion matrix represents the linear regression between the real output and the output estimated by the deep network, we note a good correlation between the values.

IV.4.2.1 Validation of results

This step consists to testing the ability of the model to generalize, to make good predictions when it is fed by data that does not belong to the original learning database.

The deep network responses which estimate the lengths of cracks are obtained by the inverse model in very short time.

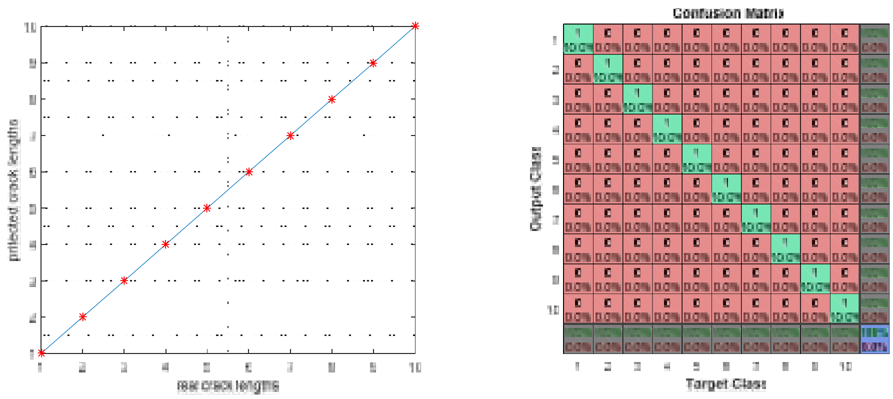

a) *b)*

Figure IV.16 - a) Estimated lengths according to the real lengths of the crack, b) correlation between the desired output and the deep network output for crack lengths

Figure IV.16 shows some of specimens that were used for the deep network validation. After comparing the targets data and deep network outputs that represent real lengths cracks and estimated lengths cracks respectively, the results of the deep neural network are very promising, where the mean square error equal to 9.1725e-13.

IV.4.3 Evaluation of the crack depths by deep network

For the evaluation of the various cracks depths (2 to 7mm), it is found that the best performance is obtained for the configurations having a minimum of 120 neurons in the first hidden layer; the optimal number of neurons for the second hidden layer is bounded lower by 120 neurons also. The deep network results are shown in the following figures:

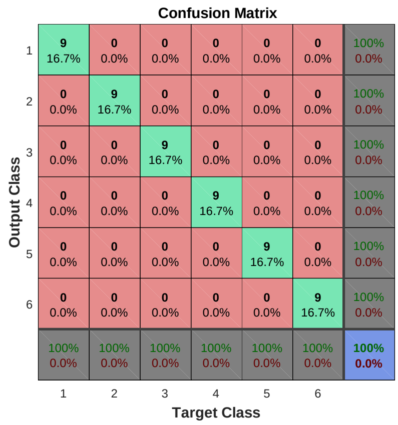

Figure IV.17 - Correlation between the desired output and the deep network output for crack depths for learning base

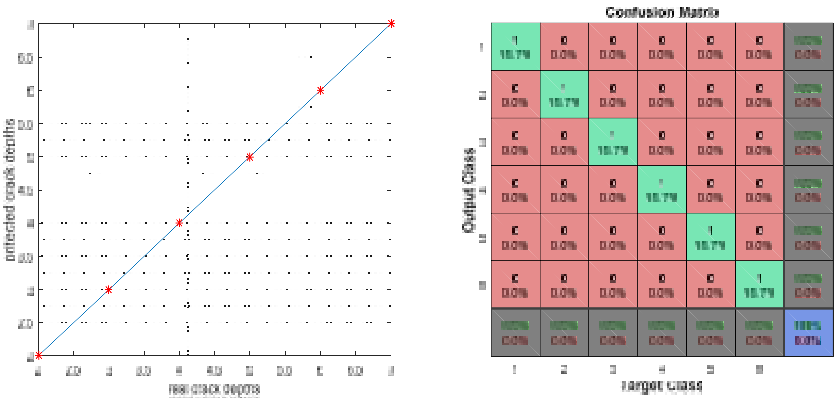

a) ***b)***

Figure IV.18 - a) Estimated depths according to the real depths of the crack, b) correlation between the desired output and the deep network output for crack depths

For the different depths of the crack, the results of the deep network show a very good accuracy and the MSE is 1.8845e-10.

IV.5 Hybrid machine learning method

The techniques of artificial intelligence based in fuzzy logic and neural networks are frequently applied together. The reasons to combine these two paradigms come out of the difficulties and inherent limitations of each isolated paradigm. Generically, when they are used in a combined way, they are called Neuro-Fuzzy Systems. This term, however, is often used to assign a specific type of system that integrates both techniques. This type of system is characterized by a fuzzy system where fuzzy sets and fuzzy rules are adjusted using input output patterns. There are several different implementations of neuro-fuzzy systems, where each author defined its own model.

Hybrid Neuro-Fuzzy System, in this category, a neural network is used to learn parameters of the fuzzy system (parameters of the fuzzy sets, fuzzy rules and weights of the rules). There are several hybrid neuro-fuzzy architectures, in this part we use the Adaptive Network based Fuzzy Inference System (ANFIS) for the crack characterization by the inversion of the problem.

IV.5.1 ANFIS architecture

The Adaptive Network based Fuzzy Inference System ANFIS implements a TAKAGI SUGENO fuzzy inference system and it has five layers as shown in figure IV.19.

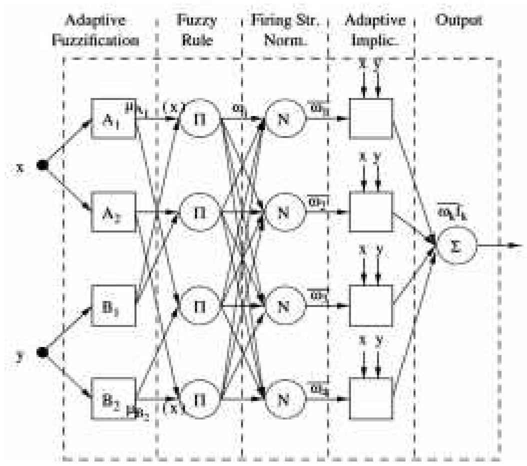

Figure IV.19 - ANFIS architecture with two inputs, one output,

and four rules

A representative ANFIS architecture with two inputs (x and y), one output (f), and four rules is illustrated in figure IV.19, which consists of five layers: adaptive fuzzification, fuzzy rule, firing strength normalization, adaptive implication, and output.

IV.5.2 ANFIS learning

Adjusting ANFIS parameters is realized during the learning phase, after the construction of ANFIS network the hybrid learning algorithm is applied. ANFIS uses mean square method to determine the consequents parameters, and the backpropagation learning to determine the membership functions parameters.

In the first part, the input patterns are propagated and the parameters of the consequents are calculated using the minimum squared method algorithm, while the parameters of the premises are considered fixed. In the second part, the learning backpropagation algorithm is used to modify the parameters of the premises, while the consequents remain fixed.

IV.5.3 Evaluation of the crack lengths by Neuro-Fuzzy system (ANFIS)

The ANFIS model can be optimized through its training process. Since the architecture was predefined, the model is optimized only in the parameter sense.

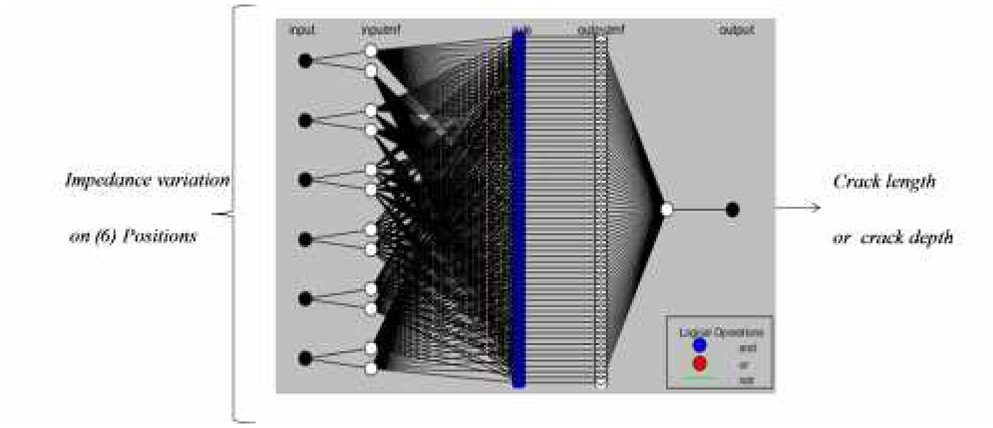

Figure IV. 20 - ANFIS architecture for the crack lengths evaluation

Our ANFIS system for the evaluation of crack lengths is zero-order TAKAGI-SUGENO type, with 6 inputs, 1 output and 2 bell membership functions per input. The ANFIS inputs represented the probe impedance variation, while its outputs represented the crack lengths.

The reason to introduce 6 impedance values to the ANFIS input instead of 21 impedance values, due to the large size of this vector (21 elements), is the out-off memory problem. Was solved this problem by the segmentation size of this large vector in sets, each one of them of six input values.

The first hidden layer is responsible for the mapping of the impedance variable relatively to each membership functions. The operator "AND" is applied in the second hidden layer to calculate the antecedents of the rules. The third hidden layer normalizes the rules strengths followed by the fourth hidden layer where the consequents of the rules are determined. The output layer calculates the global output which is the crack lengths as the summation of all the signals that arrive to this layer. The learning result is shown in the following figure:

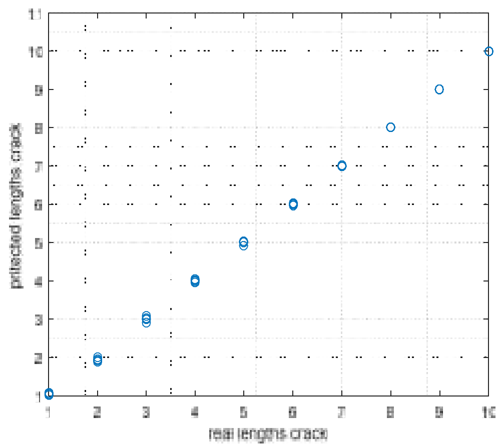

Figure IV.21 - Correlation between the desired output and the ANFIS output for crack lengths

The good correlation between the values allowed us to say that our ANFIS model has adapted its parameters well to realize the desired output.

IV.5.3.1 Validation of results

We test the ability of our ANFIS model to make good predictions when it's powered by data that does not belong to the original learning database, the figure III.22 shows the validation result.

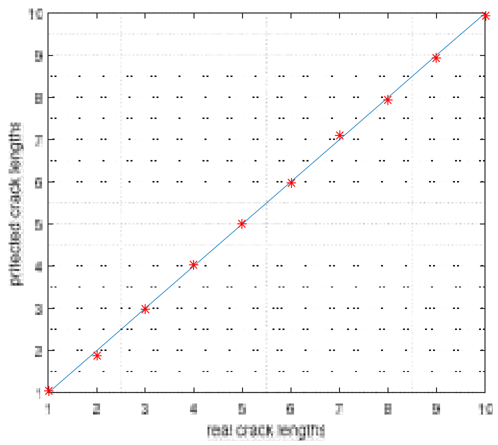

Figure IV.22 - Estimated lengths according to the real lengths of the crack for the validation database

We note that the convergence time is fast, and the MSE equals 0.0039, on the basis of these results we can conclude that the inversion by learning hybrid method (ANFIS) is able to generalize and gives results with good accuracy.

IV.5.4 Evaluation of the crack depths by Neuro-Fuzzy System (ANFIS)

To restore the different depths of the crack, for this we follow the same procedure used to restore the different lengths, the only difference is that the membership function in this case is triangular type. The learning and validation results are presented in the following figures:

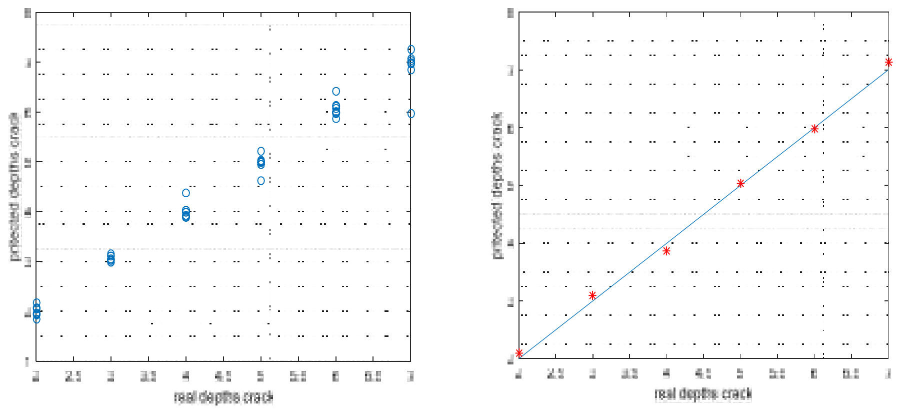

a) ***b)***

Figure IV.23 - a) Correlation between the desired output and the ANFIS output for the crack depths, b) estimated depths according to the real depths of the crack for the validation database

For our ANFIS model and for the restoration of the different crack depths, we obtain a good accuracy of calculation with 0.0093 as mean square error.

IV.6 Conclusion

In this chapter, different machine learning methods are implemented in Matlab software to characterize the crack specifically its length and depth, using these methods allowed us to solve the inverse problem. For all these learning methods, the good preparation of the learning base has a very important influence on the results that will be obtained and for this reason the sensor signature on 21 measurement points were presented as a network input, this is to ensure the uniqueness of the solution.

The first approach used to characterize the crack is the artificial neural networks PML, which allowed us to estimate with good accuracy the parameters sought once the optimal architecture is found.

The second approach used is deep learning, which gives very good results in terms of computational precision and fast convergence time, because this learning method is very intended for big data which is well suited to our input vector of important dimension.

The third approach used is the neuro-fuzzy hybrid learning method, despite the good calculation accuracy and the fast convergence time, there remains a major disadvantage due to the large size of the input vector, which leads to off-line learning, because of this problem, we divided this vector into segmentations each of 6 input elements, and by ANFIS we have learned these segmentations individually.

General Conclusion and Perspectives

General conclusion and perspectives

The detection and characterization of a defect is one of the most common problems encountered in most industrial sectors, aeronautical and nuclear, as they have been faced with the obligation to acquire the most advanced techniques, to inquire about the physical and geometrical characteristics of the different materials. This work includes a general overview of the different NDT techniques as well as the different methods of solving direct NDT problems. In order to choose the most suitable technique for an application, a number of criteria can be taken into account such as the ease of technique implementation, its low cost and its detection efficiency.

Among these non destructive testing (NDT) techniques, that of eddy currents (EC) is widely used industrially mainly because of its non-polluting character, it is very sensitive to "crack" defects located on the surface or adjacent surface of the inspected structure. In this respect, we proposed to study and solve a NDT problem by the EC technique. For the development of mathematical models describing these systems, the finite element method has been exploited to generate such a mathematical model that aims to simulate the interaction sensor-piece to be tested.

This is followed by a comparative study of the different approaches of machine learning, in particular: neural networks, deep learning and hybrid methods. In the end, an inverse model for each of these approaches has been developed in order to reconstitute the crack geometry, for different lengths and different depths from the data obtained through the direct problem elaborated in the first part. For all these learning methods, the good preparation of the learning base has a very important influence on the results that will be obtained and for this reason the sensor signature on 21 measurement points will be presented as a network input, this is to ensure the uniqueness of the solution. An important problem in the inversion process is the selection of the network structure and the adjustment of its internal parameters. In order to develop an optimal approach, we have carried out several experiments by varying the settings of the network, and the learning algorithm used.

In terms of perspectives for this work, it might be interesting to develop the learning database in order to model structures with other defects (corrosion, fatigue, wear, burn...). With regard to the second chapter, we have prepared the field of work, concerning the circuit used for the measurement, the measuring apparatus ... etc., this chapter has met problems concerning the realization of the standards with the electrical discharge machining technique at the Laghouat Maintenance Direction (LMD), another order was sent to the central logistics base in Algiers (CLB), but the latter has been delayed, the finalization of this part will be the starting point for further work.

BIBLIOGRAPHICAL REFERENCES

Bibliographical references

[ABD 06] **A. Abdou**, *Contrôle non destructif par courant de Foucault, Etude et réalisation d'un capteur inductif*, Mémoire de Magister, Spécialité électrotechnique, Option matériaux d'électrotechnique, Université de Batna, 2006.

[ALT 92] **C. von Altrock, B. Krause, H. J. Zimmerman**, *Advanced fuzzy logic control technologies in automotive applications*, Proc. IEEE Int. Conf. Of Fuzzy Systems, San Diego, 1992, pp. 835-842.

[ANA 92] **Anand, Mehrotra, Mohan, Ranka**, *Intelligent Control using Neural Networks*, IEEE Control System mag; Avril, pp 11-18, 1992.

[ASA 94] **K. Asakawa and H. Takagi**, *Neural Networks in Japan*, Communication of the ACM, Vol. 37, No. 3, 1994, pp. 106-112.

[AYO 12] **S.Ayouni**, *Etude et Extraction de Règles graduelles floues : Définition d'algorithmes efficaces*, Thèse de doctorat en cotutelle, Université Montpellier II et Université Tunis El Manar, 2012.

[BEL 03] **Y. Belkhiri**, *Modélisation des phénomènes électromagnétiques et mécaniques couples par la méthode des volumes finis (CVM)*, mémoire de magister, Spécialité électrotechnique, Université de Batna, 2003.

[BEN 06] **S. Bensaid**, *Contribution à la Caractérisation et à la Modélisation Electromagnétique et Thermique des Matériaux Composites Anisotropies*, Thèse de Doctorat, à l'IREENA Saint-Nazaire, Université de Nantes, 2006.

[BEN 09] **O. Benzaim**, *Techniques multiport pour la conception et la réalisation de systèmes micro-ondes dédiés à l'évaluation non destructive de matériaux*, thèse de doctorat, l'université de Lille 1 sciences & technologies, 2009.

[BEN 14] **N. Benhadda, T. Bouchala, A. Guettafi, B. Abdelhadi,** *Study of the Influence of Conductive Defect Characteristics on Eddy Current Differential Probe Signal*, Journal of Electrical Engineering, (JEE Romania), 2014, Issue 3.

[BIH 08] **y. Le Bihan, J. Pavo, C. Marchand**, *caracterization of small cracks in eddy current testing*, The European Physical Journal Applied Physics, vol. 43, 2008.

[BOI 94] **A. Boidin,** *Les capteurs à Courants de Foucault,* SCHENCK France, 1994.

[BOU 13] **T. Bouchala, B. Abdelhadi, A. Benoudjit,** *Novel Coupled Electric Field Method for Defect Characterization in Eddy Current non-Destructive Testing Systems*, Journal of Nondestructive Evaluation, 2013, Springer Science+ Business Media, New York, USA.

[BOU 14] **T. Bouchala**, *Développement de Méthodes Rapides pour la Résolution des Problèmes Directes dans les Systèmes de CND par Courants de Foucault*. Thèse de Doctorat, Université El-Hadj Lakhder, Batna, 2014.

[CAR 05] **M. A. Carreira-Perpinan, G.E. Hinton**, *On contrastive divergence learning*. In : AISTATS. vol. 10., Citeseer, 2005, pp. 33–40.

[CAU 05] **F. Cau, A. Fanni, A. Montisci, P. Testoni, M. Usai**, *Artificial neuron networks for Non-destructif evaluation with ultrasonic waves in not accessible pipes,* 0-7803-9208, p685-692 /IEEE Mai 2005.

[CHE 07] **A. Cheriet**, *Contribution à la modélisation tridimensionnelle par la méthode des volumes finis de dispositifs électromagnétiques,* Thèse de Doctorat, Spécialité électrotechnique, Université de Biskra, 2007.

[CHO 09] **Y. Choua**, *Application de la méthode des éléments finis pour la modélisation de configurations de contrôle non destructif par courants de Foucault*, Thèse de Doctorat, Spécialité Physique, Ecole Doctorale « Sciences et Technologies de l'Information des Télécommunications et des Systèmes », Université de Paris-Sud 11, 2009.

[COS 34] **C.R. Cosens**. *A balance-detector for alternating current bridges*, Proceedings of the Physical Society, 46:818, 1934.

[DEN 13] **L. Deng, D. Yu**, *Deep Learning: Methods and Applications*, Foundations and Trends R_ in Signal Processing, Vol. 7, Nos. 3–4 (2013) 197–387, 2013.

[DEP 03] **Lionel Depradeux**, *Simulation numérique du soudage - Acier 316L. Validation sur cas tests de complexité croissante*. Thèse de doctorat, INSA de Lyon, 2003.

[DID 92] **M. Didier**, *Utilisation d'un Réseau de Neurones Artificiels comme Fonction d'Evaluation d'un Jeu*, EPFL-DMA, CH-1015 Lausanne, 1992.

[DUM 96] **J. Dumont-fillon**, *Contrôle non destructif (CND),* technique de l'ingénieur R1400, 1996, pp. (1-42).

[HAG 94] **M.T. Hagan, M. Menhaj**, *Training feedforward networks with the Marquardt algorithm*. IEEE Transactions on Neural Networks.v.5, No.6, p989- 993, 1994.

[HAL 16] **P. Hall, W. Phan, K. Whitson**, *The Evolution of Analytics, opportunities and Challenges for Machine Learning in Business*, 2016 O'Reilly Media.

[HAL 91] **R. Halmshaw**, *Non-destructive testing***,** 2nd Ed, 1991, ISSN: 09638695.

[HEL 06] **B. Helifa, A. Oulhadj, A. Benbelghit, I.K. Lefkaier, F. Boubenider, D. Boutassouna**, *Detection and measurement of surface cracks in ferromagnetic materials using eddy current testing*, NDT&E International, Elsevier, Vol. 39, Issue 1, March 2006, pp. 384-390.

[HEL 12] **B. Helifa**, *Contribution à la simulation du CND par courants de Foucault en vue de la caractérisation des fissures débouchantes*, Thèse de Doctorat de l'Université de Nantes, 2012.

[HIN 06] **G. Hinton, S. Osindero, Y.Teh**, *A fast learning algorithm for deep belief nets*. Neural Computation., 18(7):1527-1554, July 2006.

[HUR 06] **D. Hur, D. Lee, M. Choi, U.Lee, S. Kim, J. Han**, *Discrimination method of through-wall cracks in steam generator tubes using eddy current signals*, NDT&E International 39 (2006) 361–366.

[HUR 10] **D. Hur, M. Choi, D. Lee, S. Kim, J. Han,** *A case study on detection and siz-ing of defects in steam generator tubes using eddy current testing, Nuclear Engineering and Design*, Vol. 240 (2010), pp. 204–208**.**

[IDA 83] **N. Ida, R. Palanismy, and W. Lord**, *Eddy current probe design using finite element analysis*, Materials Evaluation, Nov.pp1389-94, 1983.

[IDA 88] **N. Ida**, *Alternative approaches to the numerical calculation of impedance*. NDT International Vol 21 1 February 1988.

[JAN 93] **J. S. R. Jang**, *ANFIS: adaptive network-based fuzzy inference systems*. IEEE Trans Sys Man Cybern 23: 665–685, 1993.

[KAN 03] **H. Kanayama, D. Tagami, K. Imoto, and S. Sugimoto**, *Finite element computation of magnetic field problems with the displacement current*, Computational and Applied Mathematics, vol. 159, 2003, pp. 77–84.

[KHE 06] **M.L. Khene**, *Modélisation des phénomènes électromagnétiques dans les structures à géométries complexes par adaptation de la méthode des volumes finis*, mémoire de magister, Spécialité électrotechnique, Université de Batna, 2006.

[LON 12] **C. Long,** *Evaluation non-destructive quantitative de structures aéronautiques par la méthode des courants de Foucault*, thèse de doctorat de l'école normale supérieure de cachan, 2012.

[MIC 38] **W. C. Michels**, *A Double Tube Vacuum Tube Voltmeter*, Rev. Sci. Instrum., 9:10, 1938.

[MIC 41] **W. C. Michels, N. L. Curtis**, *A Pentode Lock in Amplifier of High Frequency Selectivity*. Rev. Sci. Instrum., 12:444, 1941.

[OZD 89] **Ozdamar, Yaylali, Tayakar, Lopez**, *Inversion of Multilayer Networks*. Int, Joint. Conf. Neural Networks, Washington, Juin, pp 425-430, 1989.

[PAV 06] **J. Pavo, D. Lesselier**, *Calculation of Eddy Current Testing Probe Signal with Global Approximation*, IEEE Transactions on Magnetics, Vol. 42, No. 4, April 2006, pp. 1419-1422.

[PEI 02] **X.-M. Pei, H.-S. Liang, Y.-M. Qia**, *A frequency spectrum analysis method for eddy current nondestructive testing*, Proceedings of the IEEE International Conference on Machine Learning and Cybernetics, Vol. 3, 2002.

[PEI 88] **G. PEIX**, *Contrôle non destructif par courant de Foucault*, I.N.S.A. de Lyon, 1988.

[PIN 87] **FJ. Pineda**, *Generalization of Back-Propagation to Recurent Neural Networks*, Physical Review letters, 59(19), pp 2229-2232,1987.

[RAM 09] **B. Ramdane**, *Contribution à la modélisation tridimensionnelle de la technique thermo-inductive de contrôle non destructif : Développement d'un outil de* *conception, d'analyse et d'aide à la décision*, Thèse de Doctorat, Spécialité électrotechnique et génie électrique, Université de Nantes, 2009.

[RAV 08] **C. Ravat**, *Conception de Multicapteurs à Courants de Foucault et Inversion des Signaux Associés pour le Contrôle non Destructif*, Thèse de Doctorat, Paris-Sud 11, 2008.

[REN 99] **Z. Ren**, *Solving 3-D eddy current problem containing thin cracks using dual formulations and shell elements*, IEE Proc.-Si. Mms. Technol., Vol. 146. No. 1, January 1999, pp. 9-14.

[ROS 57] **F. Rosenblatt**, *The perceptron a perceiving and recognizing automaton,* Tech. Report 85-460-1, Cornell Aeronautical Laboratory, Ithaca, N.Y., 1957.

[RUM 86] **D. E. Rumelhart, G.E. Hinton et RJ. Williams**, *Learning Internal Representations by error Propagation,* Parallel Distributed Processing, 1 (8), pp 319-362, 1986.

[SHA 97] **Shatat A., Atherton D. L.,** *Remote Field Eddy Current Inspection of Support plate Fretting Wear,* Materials Evaluation, March 1997,p. 3.

[SHU 02] **P.J. Shull**, *Nondestructive evaluation theory, techniques and applications,* edition Marcel Dekker, New York, 2002.

[TIE 09] **T. Tieleman, G. Hinton**, *Using fast weights to improve persistent contrastive divergence*. In: Proceedings of the 26th Annual International Conference on Machine Learning, ACM, 2009, pp. 1033–1040.

[TRI 10] **A. Trillon**, *Reconstruction de défauts à partir de données issues de capteurs à courants de Foucault avec modèle direct différentiel*, Thèse de doctorat, Université de Nantes, 2010.

[UDP 04] **S. S. Udpa**, *Non-destructive Testing Handbook- Electromagnetic testing*, Third Edition,5, ASNT, chap-4,2004.

[UTK 93] **V. l. Utkin**, *Sliding mode control design principles and applications to electric drives*, IEEE trans. Ind. Electron. 40, (1), pp. 23-36, 1993.

[VAL 07] **S. Vallamsundar**, *Numerical Evaluation of Classification Techniques for Flaw Detection*, thesis requirement for the degree of Master of Applied Science in Civil Engineering, University of Waterloo, Canada 2007.

[VIN 10] **P. Vincent, H. Larochelle, I. Lajoie, Y. Bengio, P. A. Manzagol**, *Stacked denoising autoencoders: Learning useful representations in a deep network with a local denoising criterion*, The Journal of Machine Learning Research, 2010, 11, pp. 3371–3408.

[VUI 94] **P.L. Vuillerrmoz**, *Les courants de Foucault : Principes, mesure et contrôle*, AFNOR, 1994.

[WAT 87] **R. L. Watrous**, *Learning Algorithms for Connectionist Networks: Applied Gradient Methods of Nonlinear Optimization*, IEEE First International Conference on Neural Networks, 2, pp 619-627, 1987.

[web page] Zurich Instruments HF2LI. Product web page.

[WEI 03] **M. Weinfeld**, *Réseaux de neurones*, techniques de l'ingénieur, H1990, 2003.

[YAN 98] **M. Yan, S. Udpa, M. Shreekanth, Y. Sun, S. Paul, and W. Lord**, *Solution of inverse problems in electromagnetic NDE using finite element methods*, IEEE Transactions on Magnetics, Vol.34, No 5, September 1998.

[YAS 02] **N. Yasa, W. Cheng, Z. Chen, K. Miya**, *Generalized Neural Network approach to Eddy Current Inversion for real cracks*, NDT & International 35,609-614, 2002.

[ZAD 65] **L. A. Zadeh**, *Fuzzy Sets*, Information and Control, 1965, Vol. 8, pp. 338-353.

[ZAI 12] **H. Zaidi**, Méthodologies pour la Modélisation des Couches Fines et du Déplacement en Contrôle non Destructif par Courants de Foucault : Application aux Capteurs Souples, thèse de Doctorat, Université, Paris- Sud, 2012.

[ZAO 08] **A.Zaoui**, Contribution à la Modélisation de CND par Matrice à Courants de Foucault, thèse de Doctorat, Ecole Militaire Polytechnique, Alger, Octobre 2008.

Abstract

The study of determining the defects profile in metallic structures using non destructive testing (NDT) techniques still presents enormous relevance in the current scenario, mostly in managing cost, efficiency and security of industry components. The main goal of this work consists in the cracks characterization. In this work, the measurement system is based on the eddy currents testing (EC), which is a well-established and reliable NDT technique used in several domains. Experimental tests were performed using, in the vicinity of the plate, an excitation coil driven by a sinusoidal current, with fixed amplitude, generating an associated magnetic field. Thus, eddy currents are induced within the metal sample and create a secondary magnetic field. The presence of cracks changes the normal path of the eddy currents.

A database based on an experimental analysis and a finite element modeling made it possible to build a direct 3D model. Through that database, we investigate different machine learning methods to reconstruct the length and depth of the defect, in order to obtain a characterization of the crack that leads to the resolution of the inverse problem.

Keywords: Non destructive testing, eddy currents, crack characterization, inverse problem machine learning, artificial neuron network.

Résumé

L'étude de la détermination du profil des défauts dans les structures métalliques en utilisant les techniques de contrôle non destructif (CND) continue d'être extrêmement pertinente dans le scénario actuel, principalement dans la gestion du coût, de l'efficacité et de la sécurité des composants de l'industrie. L'objectif principal de ce travail consiste à la caractérisation des fissures. Dans ce travail, le système de mesure est basé sur le contrôle par courants de Foucault (CF), qui est une technique de CND bien établie et fiable utilisée dans plusieurs domaines. Des tests expérimentaux ont été réalisés à l'aide d'une bobine d'excitation pilotée par un courant sinusoïdal à amplitude fixe, à proximité d'une plaque, générant un champ magnétique associé. Ainsi, les courants de Foucault sont induits dans l'échantillon de métal et créent un champ magnétique secondaire. La présence de fissures change la voie normale des courants de Foucault.

Une base de données basée sur une analyse expérimentale et une modélisation d'éléments finis permettait de construire un modèle direct 3D. Grâce à cette base de données, nous étudions différentes méthodes d'apprentissage automatique pour reconstruire la longueur et la profondeur du défaut, afin d'obtenir une caractérisation de la fissure qui mène à la résolution du problème inverse.

Mots-clés : contrôle non destructif, courants de Foucault, caractérisation de la fissure, problème inverse, apprentissage automatique, réseau de neurones artificiels.